Journal of Applied Mathematics and Computing (2026) 72:35
https://doi.org/10.1007/s12190-025-02687-7

ORIGINAL RESEARCH

Nonlinear dynamical modeling and control of Ebola involving transmission from hospitalized and deceased populations: a data-driven approach from Sierra Leone

Qiuni Zhu[1] · Muhammad Asim[2] · Saif Ullah[2,3] · Sabila[2] · Arshad Alam Khan[2]

Received: 4 August 2025 / Revised: 16 September 2025 / Accepted: 18 September 2025

Abstract

The Ebola virus continues to present major public health concerns, particularly in African countries including Sierra Leone. Transmission of Ebola virus from deceased and hospitalized people significantly contributed to the disease outbreak in these regions. This study introduces a novel compartmental model designed to understand the dynamical patterns and to explore optimal control intervention for managing the spread of Ebola with transmission from deceased people. The model incorporates vaccinated and hospitalized population groups one of the most effective preventive interventions. Global dynamics of the model is assessed using Lyponov approach to evaluate the stability of the system's equilibria. The model is validated using the reported daily cases in Sierra Leone during the severe outbreak and the numerical values of the basic reproduction number is estimated. The parameter estimation carried out via the nonlinear standard least squares method. A comprehensive sensitivity analysis is conducted to identify critical parameters that influence disease progression and informs the design of effective time-dependent control interventions. Moreover, the model is optimized using Pontryagin Maximum Principle to suggest the optimal intervention for the infection eradication. Simulation shows that applying a combination of the three suggested time-dependent controls significantly reduces the number of infected and exposed cases, while maximizing the number of hospitalized and vaccinated individuals. Among these, continuous treatment of infectious individuals, especially when paired with early vaccination, proves to be the most effective long-term measure. The results highlight the value of prompt and strategic public health actions in curbing Ebola outbreaks.

Keywords Ebola modeling · Transmission from deceased and hospitalized class · Estimation with real data · Pontryagin maximum principle · Simulation

Extended author information available on the last page of the article

Published online: 01 December 2025

1 Introduction

Infectious diseases are caused by harmful microorganisms such as bacteria, viruses, parasites, and fungi. These illnesses can spread through various transmission routes, including direct contact between people, transmission from animals to humans, or even among animals before eventually affecting humans. Reverse zoonosis occurs when a disease is passed from humans to animals, usually through another species acting as a carrier. Worldwide one-third of all deaths are attributed to infectious diseases. Recent outbreaks of emerging diseases present significant risks to both public health and the global economy [1]. The symptoms of infectious diseases vary based on the type of infection. Fungal infections often affect certain parts of the body, causing issues like rashes and itching. In contrast, viral and bacterial infections can lead to symptoms that affect multiple areas of the body, such as chills, digestive issues (diarrhea, vomiting, nausea), cough, fatigue, fever, headache, muscle aches, and a runny or stuffy nose.

Ebola is a severe hemorrhagic fever that affects humans and can be fatal. It is typically caused by a virus from the *Filoviridae* family [2]. The case fatality rate varies between 25 and 90%, depending on the strain of the virus [3]. Infection typically begins with a spill over event from an animal host to a human. After this initial transmission, the virus can spread between people, potentially causing widespread outbreaks. Ebola Virus Disease (EVD) transmit via direct interaction with the blood and other bodily fluids of an infectious person including those who have died from the illness. Transmission can occur through broken skin or mucous membranes in areas like the eyes, nose or mouth [4]. Over the past few decades, Africa has experienced more than 20 EVD outbreaks, triggered by various strains of the ebola virus. According to the Centers for Disease Control and Prevention (CDC), 2017, there are five distinct strains of ebolaviruses, but the three most deadly are the Zaire, Sudan, and Bundibugyo strains. A Central African virus may have spread to West Africa through migratory bats that can travel hundreds of kilometers, according to one theory among many that explain the infection's spread [5]. Outbreaks of EVD are driven not only by direct transmission between individuals but also by a complex interplay of environmental, social, and economic conditions. Additionally, behavioral changes driven by fear can significantly impact how the disease spreads. Among the numerous questions that remain unanswered about this virus are its natural host and how humans are initially infected [6].

Sierra Leone was one of the three West African nations, along with Guinea and Liberia, heavily affected by the EVD 2014 outbreaks. From 2014 to 2015, Sierra Leone experienced more than 14,000 confirmed cases with infections and nearly 4000 deaths, making it a central hotspot of the epidemic. The rapid spread was caused by week healthcare infrastructure, cultural practices such as unsecured burials, and extensive population movement across the countries. The World Health Organization declared this region free of Ebola in November 2015, although sporadic cases continued to appear into 2016 [7].

The formulation of novel mathematical models and robust computational techniques serves as a valuable tool for understanding the dynamic aspects of epidemic outbreaks [8–11]. These models are usually formulated with the help of ordinary

[12, 13], fractional [14, 15], fractal-fractional [16] or stochastic [17] differential systems. These models also play a crucial role in designing effective and optimal control interventions to curb the spread of infection [18–20]. Various mathematical frameworks have been proposed to investigate the spread of the Ebola virus, and some of these models include compartments representing deceased individuals [21]. A dynamical study and prevention strategies of EVD with low and high risk susceptibility was presented in [22]. Nonetheless, only a few studies have addressed the potential for infection arising from contact with unburied bodies or the impact of transmission occurring within hospital settings. Recognizing the importance of these under represented factors, this study introduces an enhanced compartmental model that accounts for the transmission contributions of both hospitalized patients and deceased individuals [23]. Some recent mathematical models exploring Ebola dynamics and control can be found in [24–27].

1.1 Key highlights

In this study, we focus on formulating a deterministic mathematical model with optimal control analysis to assess the transmission dynamics and mitigation of Ebola infection. Furthermore, real epidemiological data are employed to support the model and optimal control outcomes. We used the 2015 data for parameter estimation because the 2014–2016 EVD outbreak in Sierra Leone was the largest and most well-documented epidemic in Ebola disease history.

Key contributions of this study include

- Formulation of a novel mathematical model to assess the transmission dynamics of Ebola, incorporating hospitalization and imperfect vaccination.
- Validation of the model using weekly reported Ebola cases from Sierra Leone during the severe outbreak.
- Analyzing the global dynamics of the model equilibria using Lyapunov stability techniques.
- Performing simulations and normalized sensitivity analysis to identify the most influential parameters affecting disease spread and control.
- Optimizing the model and designing effective control interventions through comprehensive simulation.

1.2 Structure of the study

This study is structured in 8 section detailed as follows: Sect. 2 introduces the model along with comprehensive descriptions of the parameters involved. Section 3 presents the analytical study of the model, ensuring that the system remains positive and bounded. In Sect. 4, we derive the basic reproduction number and examine the equilibrium states and their stability properties. Section 5 focuses on estimating key model parameters using data from the 2015 Ebola outbreak in Sierra Leone and includes a sensitivity analysis to assess parameter influence. Section 6 develops an optimal control framework guided by Pontryagin Maximum Principle. Section 7 covers simulation of the control control model under different intervention strategies.

2 Model description

In this study, we develop a compartmental model to describe the spread of EVD in a human population, incorporating vaccination, hospitalization, and delayed in burial practices. The model divides the entire population $N(t)$, into seven subgroups: susceptible individuals $S(t)$, vaccinated individuals $V(t)$, exposed individuals $E(t)$ who are infected but not yet infectious, infectious individuals $I(t)$ who display clinical symptoms, hospitalized individuals $H(t)$, recovered individuals $R(t)$, and deceased individuals $D(t)$ who have died from the disease but are not yet buried. The actively interacting population consists of all compartments except the deceased, hence $N(t) = S(t) + V(t) + E(t) + I(t) + H(t) + R(t)$. Newborns are recruited into the population at a rate Λ, of which a fraction $\rho \in (0, 1)$ is unvaccinated and enters the susceptible class, while the remaining proportion $1 - \rho$ is vaccinated upon entry and joins the vaccinated compartment. Individuals in both susceptible and vaccinated groups are at risk of infection through contact with individuals in the infectious, hospitalized, or deceased compartments. The rate at which susceptible individuals become exposed is described by the force of infection $\lambda(t)$, given by: $\lambda(t) = \frac{\beta_1 I(t)+\beta_2 D(t)+\beta_3 H(t)}{N(t)}$, where β_1, β_2, and β_3 represent the respective effective transmission rates from infectious individuals, deceased individuals, and hospitalized individuals. Vaccination provides partial immunity, represented by a vaccine efficacy parameter $\eta \in [0, 1]$. This means that vaccinated individuals may still become infected, but at a reduced rate $\eta\lambda(t)$ (where $\lambda(t)$ is the force of infection). Once exposed, individuals transition from the exposed class $E(t)$ to the infectious class $I(t)$ at a progression rate σ, corresponding to an average latent period of $1/\sigma$ time units. Infectious individuals may either be hospitalized at a rate ϕ, die due to the disease, or recover. The rate at which individuals leave the infectious compartment is γ_1, where a fraction $\delta \in (0, 1)$ of individuals die and move to the deceased class, and the remaining fraction $1 - \delta$ recover and join the recovered class $R(t)$. Hospitalized individuals also exit their compartment at rate γ_2, with possible outcomes of recovery or death, moving to either $R(t)$ or $D(t)$, respectively. Individuals in the deceased class are buried at rate α, where $1/\alpha$ represents the average time until burial. All living individuals are also subject to a natural mortality rate μ.

This model structure captures key epidemiological processes relevant to Ebola transmission, including exposure through contact with symptomatic, hospitalized, and deceased individuals, waning vaccine protection, and delays in safe burial. Definitions and descriptions of all parameters involved in the model are provided in Table 1 while the flow among different population groups are shown in Fig. 1. The mathematical equations governing the EVD model are formulated by the system as follows:

Table 1 Model parameters and their descriptions

Parameter	Description
Λ	Birth rate
ρ	Proportion of newborns who remain unvaccinated
μ	Natural mortality rate
β_1	Transition rate from infectious individuals showing symptoms
β_2	Flow rate from unburied deceased individuals
β_3	Transmission rate from hospitalized patients
η	Effectiveness of the vaccine
σ	Number of people exposed to infection
$\frac{1}{\gamma_1}$	Average duration an individual remains infectious
γ_2	Recovery rate from the hospitalized class
α	Rate of burial for deceased individuals
ϕ	Hospitalization rate of infectious individuals
δ	Fraction of individuals who die from EVD
v	Vaccination rate among the adult population

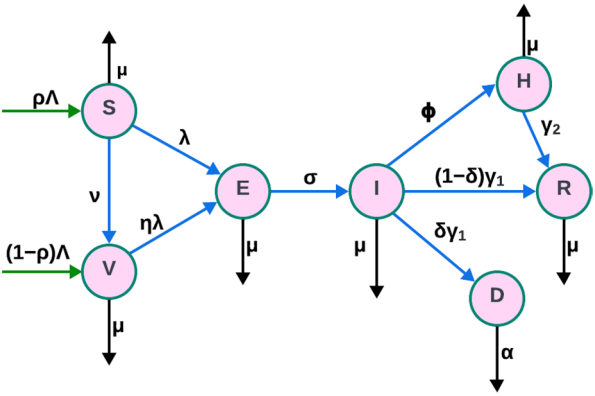

Fig. 1 Schematic diagram of the transmission dynamics. Green arrows represent recruitment into the susceptible and vaccinated classes, black arrows denote natural or disease-induced deaths, and blue arrows indicate transitions between epidemiological compartments. Notably, vaccinated individuals can still become exposed through breakthrough infections at a reduced rate (η), represented by the arrow from V to E

$$\begin{cases} S'(t) &= \rho\Lambda - \frac{(\beta_1 I+\beta_2 D+\beta_3 H)S}{N} - \nu S - \mu S, \\ V'(t) &= (1-\rho)\Lambda + \nu S - \frac{\eta(\beta_1 I+\beta_2 D+\beta_3 H)V}{N} - \mu V, \\ E'(t) &= \frac{(\beta_1 I+\beta_2 D+\beta_3 H)(S+\eta V)}{N} - (\mu+\sigma)E, \\ I'(t) &= \sigma E - (\phi+\mu+\gamma_1)I, \\ H'(t) &= \phi I - (\gamma_2+\mu)H, \\ R'(t) &= (1-\delta)\gamma_1 I + \gamma_2 H - \mu R, \\ D'(t) &= \delta\gamma_1 I - \alpha D. \end{cases} \tag{1}$$

The initial values of state variables in system 1 are:

$$S_0 > 0,\ E(0) = E_0 \geq 0,\ H(0) = H_0 \geq 0,\ I(0) = I_0 \geq 0,\ V(0) = V_0,\ R(0) = R_0 \geq 0,\ D(0) = D_0 \geq 0.$$

We observe that the presumption that older people should not receive vaccinations is not just technical: for a number of childhood illnesses, vaccinations are nearly always

administered within a brief period after birth and older people receive very little immunization [25]. For simplicity, we denote

$$K_1 = \sigma + \mu, \quad K_2 = \phi + \gamma_1 + \mu, \quad K_3 = \gamma_2 + \mu,$$

as defined in System (1).

$$\begin{cases} S' &= \rho\Lambda - \lambda S - \mu S, \\ V' &= (1-\rho)\Lambda - \lambda V - \mu V, \\ E' &= \lambda(S + \eta V) - K_1 E, \\ I' &= \sigma E - K_2 I, \\ H' &= \phi I - K_3 H, \\ R' &= (1-\delta)\gamma_1 I + \gamma_2 H - \mu R, \\ D' &= \delta\gamma_1 I - \alpha D. \end{cases} \tag{2}$$

3 Basic mathematical analysis of model

3.1 Positivity and boundedness

To analyze the behavior of system (2), it is essential to demonstrate that all state variables remain non-negative for all time, and that any solution starting with non-negative initial conditions remains within a biologically feasible and positively invariant region. This leads to the following result.

Lemma 1 *All solutions (2) with non-negative initial values remain bounded and persist in the positively invariant region defined as* $\Gamma = \{S, V, E, I, H, R, D \in \mathbb{R}_+^7 : 0 < N \leq \frac{\Lambda}{\mu}\}$.

Proof The total population of the human compartments, defined as $N(t) = S(t) + V(t) + E(t) + I(t) + H(t) + R(t)$, associated with system (1) is given by

$$\begin{aligned} N'(t) &= S'(t) + V'(t) + E'(t) + I'(t) + H'(t) + R'(t), \\ &= \Lambda - \mu\big(S(t) + V(t) + E(t) + I(t) + H(t) + R(t)\big) - \delta\gamma_1 I(t), \\ &\leq \Lambda - \mu N(t). \end{aligned} \tag{3}$$

Assuming the initial total population is given by $N(0) = N_0$, the cumulative population at time t satisfies the inequality:

$$N(t) \leq \frac{\Lambda}{\mu} - \left(\frac{\Lambda}{\mu} - N_0\right) e^{-\mu t}. \tag{4}$$

This implies that for all $t>0$, the total population remains bounded above by $\frac{\Lambda}{\mu}$. With this bound established, we proceed to reformulate the last equation in system (2) as follows:

$$D'(t) \leq \delta\gamma_1 \frac{\Lambda}{\mu} - \alpha D(t). \tag{5}$$

By applying a similar bounding technique as previously discussed, it can be shown that the number of deceased individuals satisfies the inequality $D(t) \leq \frac{\Lambda\delta\gamma_1}{\alpha\mu}$ for all $t>0$. This confirms that the model remains confined within a positively invariant region. □

Lemma 2 *Assume that $Q(0) \geq 0$ represents the initial solution and $Q(0) = (S(0), V(0), E(0), I(0), H(0), R(0), D(0))$ denote the variables of the system. Then all solutions associated with the system remain nonnegative for each time $t>0$.*

Proof Consider $t_1 = \sup\{t > 0 : Q(t) > 0,\ Q(t) \in [0, t_1]\}$. From the first equation of system (2), we get:

$$\frac{dS}{dt} = \rho\Lambda - \big(\lambda(t) + \mu\big)S. \tag{6}$$

Eq. (6) can be written in the form

$$\frac{dS}{dt} + \big(\lambda(t) + \mu\big)S = \rho\Lambda. \tag{7}$$

Using the integrating factor, we have

$$\frac{d}{dt}\left(S(t)\exp\Big(\int_0^t \mu + \lambda(x)\,dx\Big)\right) = \rho\Lambda\exp\Big(\int_0^t \mu + \lambda(x)\,dx\Big).$$

Hence,

$$S(t_1)\exp\Big(\mu t_1 + \int_0^{t_1} \lambda(x)\,dx\Big) - S(0) = \int_0^{t_1} \rho\Lambda\exp\Big(\int_0^z \mu + \lambda(x)\,dx\Big)\,dz.$$

Therefore,

$$\begin{aligned} S(t_1) = S(0)\exp\Big(-\mu t_1 - \int_0^{t_1} \lambda(x)\,dx\Big) + \exp\Big(-\mu t_1 - \int_0^{t_1} \lambda(x)\,dx\Big) \\ \times \Big(\int_0^{t_1} \rho\Lambda\exp\Big(\int_0^z \mu + \lambda(x)\,dx\Big)\,dz\Big) > 0. \end{aligned}$$

Thus, $S(t) > 0$ on $(0, t_1]$. By applying the same procedure to the remaining compartments, we obtain $V(t) > 0$, $E(t) > 0$, $I(t) > 0$, $H(t) > 0$, $R(t) > 0$, and $D(t) > 0$ for all $t \in (0, t_1]$. Consequently, every solution of system (2) remains positive for all $t > 0$. □

3.2 Basic reproduction number

To calculate the basic reproduction number R_0 for system (2), we adopt the standard next-generation matrix method as outlined in [28, 29]. In this framework, the infectious states are identified as the compartments E, I, H, and D. System (2) admits a unique disease-free equilibrium (DFE), given by

$$E_0 = \left(\frac{\rho\Lambda}{\mu}, \frac{(1-\rho)\Lambda}{\mu}, 0, 0, 0, 0, 0 \right). \tag{8}$$

By substituting the relevant components of DFE E_0 into the system, we obtain the Jacobian matrix F corresponding to the new infection terms as:

$$F = \begin{pmatrix} 0 & (\eta(1-\rho)+\rho)\,\beta_1 & (\rho+\eta(1-\rho))\,\beta_3 & (\rho+\eta(1-\rho))\,\beta_2 \\ 0 & 0 & 0 & 0 \\ 0 & 0 & 0 & 0 \\ 0 & 0 & 0 & 0 \end{pmatrix},$$

and the Jacobian matrix V, which corresponds to the transition terms (i.e., the movement between compartments other than new infections), is given by:

$$V = \begin{pmatrix} K_1 & 0 & 0 & 0 \\ -\sigma & K_2 & 0 & 0 \\ 0 & -\phi & K_3 & 0 \\ 0 & -\delta\gamma_1 & 0 & \alpha \end{pmatrix},$$

According to the method described in [28, 29], the basic reproduction number R_0 is defined as the spectral radius of the matrix product FV^{-1}. Thus, we have:

$$R_0 = \frac{(\eta(1-\rho)+\rho)\,\sigma\,(\alpha\phi\beta_3 + K_3\,(\alpha\beta_1 + \delta\beta_2\gamma_1))}{\alpha K_1 K_2 K_3}.$$

We have split R_0 into three subparts.

$$R_{01} = \frac{(\rho+\eta(1-\rho))\,\sigma\,\phi\,\beta_3}{K_1\,K_2\,K_3}.$$

$$R_{02} = \frac{(\rho+\eta(1-\rho))\,\sigma\,\beta_1}{K_1\,K_2}.$$

$$R_{03} = \frac{(\rho+\eta(1-\rho))\,\sigma\,\delta\,\beta_2\,\gamma_1}{\alpha\,K_1\,K_2}.$$

The basic reproduction number can be split into three components corresponding to distinct transmission pathways. R_{01} accounts for infections caused by hospitalized infected individuals as it assumed that even though hospitalized individuals are under medical care, they may yet contribute to Ebola transmission. R_{02} represents direct transmission from active Ebola infected individuals in the community, while R_{03} quantifies infections transmitted via deceased individuals, reflecting indirect post-mortem transmission. This decomposition highlights the relative contribution of each route, indicating that controlling community spread reduces R_{02}, improving isolation and treatment limits R_{01}, and safe handling of deceased individuals mitigates R_{03}, providing a focused basis for intervention strategies.

4 Analysis of equilibrium points and stability

For the proposed model (2), we determine the conditions for the existence of an endemic steady state [30]. We denote the endemic steady state by $E_1 = (S^*, V^*, E^*, I^*, H^*, R^*, D^*)$, and it is derived as follows:

$$\begin{cases} S^* = \frac{\Lambda\rho}{\lambda^*+\mu}, \\ V^* = \frac{\Lambda(1-\rho)}{\eta\lambda^*+\mu}, \\ E^* = \frac{\lambda^*(\eta\lambda^*\Lambda+\eta\Lambda\mu+\Lambda\mu\rho-\eta\Lambda\mu\rho)}{(\lambda^*+\mu)(\eta\lambda^*+\mu)K_1}, \\ H^* = \frac{\lambda^*(\eta\lambda^*\Lambda+\eta\Lambda\mu+\Lambda\mu\rho-\eta\Lambda\mu\rho)\sigma\phi}{(\lambda^*+\mu)(\eta\lambda^*+\mu)K_1K_2K_3}, \\ R^* = \frac{\lambda^*(\eta\lambda^*\Lambda+\eta\Lambda\mu+\Lambda\mu\rho-\eta\Lambda\mu\rho)\sigma(K_3\gamma_1-\delta K_3\gamma_1+\phi\gamma_2)}{\mu(\lambda^*+\mu)(\eta\lambda^*+\mu)K_1K_2K_3}, \\ D^* = \frac{\delta\lambda^*(\eta\lambda^*\Lambda+\eta\Lambda\mu+\Lambda\mu\rho-\eta\Lambda\mu\rho)\sigma\gamma_1}{\alpha(\lambda^*+\mu)(\eta\lambda^*+\mu)K_1K_2}, \\ I^* = \frac{\lambda^*(\eta\lambda^*\Lambda+\eta\Lambda\mu+\Lambda\mu\rho-\eta\Lambda\mu\rho)\sigma}{(\lambda^*+\mu)(\eta\lambda^*+\mu)K_1K_2}. \end{cases} \tag{9}$$

To compute the infection force λ^*, we substitute the equilibrium variables into the following expression:

$$\lambda^* = \frac{\beta_1 I^* + \beta_2 D^* + \beta_3 H^*}{N^*}. \tag{10}$$

After simplification, the resulting expression is:

$$A{\lambda^*}^2 + B\lambda^* + C = 0. \tag{11}$$

$$\begin{aligned} A &= \eta\Big(K_3\big(\alpha\mu\sigma + \alpha\mu K_2 + (\alpha(1-\delta)+\delta\mu)\sigma\gamma_1\big) + \alpha\sigma\phi(\mu+\gamma_2)\Big), \\ B &= \mu(1-R_0) + \mu\Big(K_3\big(\alpha(\mu(\rho+(1-\rho)\eta) - (1-\eta)\rho K_1)K_2 \\ &\quad + (\eta+(1-\eta)\rho)\sigma(\mu\alpha + ((1-\delta)\alpha+\delta\mu)\gamma_1)\big) \\ &\quad + \alpha(\rho+(1-\rho)\eta)\sigma\phi(\mu+\gamma_2)\Big), \\ C &= \mu^2(1-R_0). \end{aligned} \tag{12}$$

Theorem 4.1 *The conditions for the existence of endemic equilibria of model (2) are characterized as follows:*

(a) *A unique endemic equilibrium exists when $C<0$, which is equivalent to the condition $R_0 > 1$.*
(b) *A unique endemic equilibrium also exists if $B<0$, and either $C=0$ or the discriminant satisfies $B^2 - 4AC = 0$.*
(c) *The model admits two distinct endemic equilibria when $C>0$, $B<0$, and the discriminant condition $B^2 - 4AC > 0$ holds.*
(d) *No endemic equilibrium exists in all other cases.*

Proof According to condition (a), the model admits a unique Ebola Virus endemic equilibrium, confirming the existence of a single endemic state under the given criteria. □

4.1 Local stability of the dfe

Theorem 4.2 *The DFE $E_0\left(\frac{\Lambda\rho}{\mu}, \frac{(1-\rho)\Lambda}{\mu}, 0, 0, 0, 0, 0\right)$ is locally asymptotically stable $R_0 < 1$. Conversely, the equilibrium becomes unstable when $R_0 > 1$.*

Proof To analyze the local stability of the disease-free equilibrium, we evaluate the Jacobian matrix of system (2) at E_0. The resulting Jacobian takes the following form:

$$W = \begin{pmatrix} -\mu & 0 & 0 & -\rho\beta_1 & -\rho\beta_3 & 0 & -\rho\beta_2 \\ 0 & -\mu & 0 & -\eta(1-\rho)\beta_1 & -\eta(1-\rho)\beta_3 & 0 & -\eta(1-\rho)\beta_2 \\ 0 & 0 & -K_1 & \frac{\mu\left(\frac{\eta\Lambda(1-\rho)}{\mu}+\frac{\Lambda\rho}{\mu}\right)\beta_1}{\Lambda} & \frac{\mu\left(\frac{\eta\Lambda(1-\rho)}{\mu}+\frac{\Lambda\rho}{\mu}\right)\beta_3}{\Lambda} & 0 & \frac{\mu\left(\frac{\eta\Lambda(1-\rho)}{\mu}+\frac{\Lambda\rho}{\mu}\right)\beta_2}{\Lambda} \\ 0 & 0 & \sigma & -K_2 & 0 & 0 & 0 \\ 0 & 0 & 0 & \phi & -K_3 & 0 & 0 \\ 0 & 0 & 0 & (1-\delta)\gamma_1 & \gamma_2 & -\mu & 0 \\ 0 & 0 & 0 & \delta\gamma_1 & 0 & 0 & -\alpha \end{pmatrix}.$$

From the structure of matrix W, it is clear that the eigenvalue $-\mu$ with multiplicity 3 is negative. The remaining eigenvalues are determined from the submatrix associated with the infectious classes. If $R_0 < 1$, all eigenvalues of the Jacobian have negative real parts, implying that the DFE is locally asymptotically stable. On the other hand, if $R_0 > 1$, the matrix has at least one eigenvalue with positive real part, and the equilibrium becomes unstable.

$$C_0\lambda^4 + C_1\lambda^3 + C_2\lambda^2 + C_3\lambda + C_4 = 0. \tag{13}$$

The coefficients present in Eq. (13) are as follows:

$$
\begin{aligned}
&C_0 = 1,\\
&C_1 = \alpha + K_1 + K_2 + K_3,\\
&C_2 = K_1K_2(1 - R_{01}) + \alpha(K_1 + K_2) + K_3(K_2 + \alpha + K_1),\\
&C_3 = \alpha K_1K_3 + \alpha K_2K_3 + \alpha K_1K_2(1 - R_{01} - R_{02}) + K_1K_2K_3(1 - R_{01} - R_{03}),\\
&C_4 = \alpha K_1K_2K_3(1 - R_0).
\end{aligned}
$$

It can be observed that all coefficients C_j (for j=1,2,3,4,) are positive when the basic reproduction number satisfies $R_0 < 1$. In addition, the final Routh Hurwitz condition corresponding to the fourth degree characteristic polynomial given in Eq. (13) is readily satisfied under this assumption. Consequently, we conclude that the DFE is locally asymptotically stable whenever $R_0 < 1$. □

4.2 Global stability of the disease-free state

Theorem 4.3 *The DFE* $E_0\left(\frac{\Lambda\rho}{\mu}, \frac{(1-\rho)\Lambda}{\mu}, 0, 0, 0, 0, 0\right)$ *is globally asymptotically stable within the region* $\Gamma = \{(S, V, E, I, H, R, D) \in \mathbb{R}_+^7\}$ *provided that* $R_0 < 1$.

Proof To establish the global stability of the DFE, we consider the following Lyapunov function as follows [31].

$$B(t) = C_1E + C_2I + C_3H + C_4D. \tag{14}$$

The constants C_i for $i = 1, 2, \ldots, 4$ are assumed to be positive and need to be calculated. By computing the time derivative of the Lyapunov function $B(t)$ and substituting the corresponding expressions from system (2), we arrive at the following

$$
\begin{aligned}
\frac{dB(t)}{dt} =& C_1\left(\frac{\beta_1 I + \beta_2 D + \beta_3 H}{N}(S + \eta V) - K_1E\right) + C_2(\sigma E - K_2I)\\
&+ C_3(\phi I - K_3H) + C_4(\delta\gamma_1 I - \alpha D),\\
\frac{dB(t)}{dt} =& \left(\frac{C_1\beta_1}{N}(S + \eta V) - C_2K_2 + C_3\Phi + C_1\delta\gamma_1\right) I,\\
&+ \left(\frac{C_1\beta_2(S + \eta V)}{N} - C_4\alpha\right) D\\
&+ \left(\frac{C_1\beta_3(S + \eta V)}{N} - C_3K_3\right) H\\
&+ (C_2\sigma - C_1K_1)\, E,\\
\frac{dB(t)}{dt} \leq& (C_1\beta_1\,(\eta(1 - \rho) + \rho) - C_2K_2 + C_3\Phi + C_4\delta\gamma_1)\, I,\\
&+ (C_1\beta_2\,(\rho + \eta(1 - \rho)) - C_4\alpha)\, D,\\
&+ (C_1\beta_3\,(\rho + \eta(1 - \rho)) - C_3K_3)\, H,\\
&+ (C_2\sigma - C_1K_1)\, E,
\end{aligned}
$$

Now choosing the Value of constant $C_1,\ C_2,\ C_3,\ C_4$ as follows

$$C_1 = \frac{\sigma\alpha K_3}{\alpha K_1 K_3},\quad C_2 = 1,\quad C_3 = \frac{(\eta(1-\rho)+\rho)\sigma\alpha\beta_3}{\alpha K_1 K_3},\quad C_4 = \frac{(\eta(1-\rho)+\rho)\sigma K_3\beta_2}{\alpha K_1 K_3}.$$

After putting above values and some simplification, we get

$$B'(t) = K_2\,(R_0 - 1)\,I(t). \tag{15}$$

Thus, it is clear that if $R_0 < 1$, then $\frac{dB(t)}{dt} < 0$. Therefore, the only compact invariant set contained in Δ is the singleton set W. By applying LaSalle Invariant Principle [32], we can conclude that E_0 is stable globally in Γ. □

4.3 Global stability of endemic equilibrium

$$\begin{cases} \rho\Lambda & = (\lambda_1^* + \mu)S^*, \\ (1-\rho)\Lambda & = (\lambda_1^* + \mu)V^*, \\ K_1E^* & = \lambda_1^*(S^* + \eta V^*), \\ K_2I^* & = \sigma E^*, \\ K_3H^* & = \phi I^*, \\ \alpha D^* & = \delta\gamma_1 I^*. \end{cases} \tag{16}$$

and

$$\lambda_1^* = (\beta_1 I + \beta_2 D + \beta_3 H). \tag{17}$$

Theorem 4.4 *In the set $\Gamma = (S(t), V(t), E(t), I(t), H(t), R(t), D(t)) \in \mathbb{R}_+^7$ whenever $R_0 > 1$, the endemic steady state $E_1 = (S^*, V^*, E^*, I^*, H^*, R^*, D^*)$ is globally asymptotically stable.*

Proof To investigate the endemic equilibrium global stability, we suppose that the Lyapunov function $V(t)$ has the following form

$$\begin{aligned} U(t) = {} & \left(\frac{S}{S^*} - 1 - \ln\frac{S}{S^*}\right)\frac{S^*}{E^*} + \left(\frac{V}{V^*} - 1 - \ln\frac{V}{V^*}\right)\frac{V^*}{E^*} \\ & + \left(\frac{E}{E^*} - 1 - \ln\frac{E}{E^*}\right) + \frac{(I^*\beta_1 + \beta_2 D^* + \beta_3 H^*)\,(S^* + V^*\eta)\,I^*}{\sigma(E^*)^2}\left(\frac{I}{I^*} - \ln\frac{I}{I^*} - 1\right) \\ & + \frac{\beta_3\,(S^* + \eta V^*)\,(H^*)^2}{\phi E^* I^*}\left(\frac{H}{H^*} - 1 - \ln\frac{H}{H^*}\right) + \frac{\beta_2\,(S^* + \eta V^*)\,D^{*2}}{\gamma\delta E^* I^*}\left(\frac{D}{D^*} - \ln\frac{D}{D^*} - 1\right). \end{aligned}$$

Considering the function y define from $\mathbb{R} \to \mathbb{R}$ by $y(h) = 1 - h + \ln(h)$. For all positive h, the inequality $y(h) \le 0$ holds true, with equality only at $h = 1$. This implies

that for any $h>0$, the relation $h-1\geq \ln h$ is satisfied. Next, we compute the time derivative of the Lyapunov function along the trajectories of the system as follows

$$\begin{aligned}U'(t)=&\frac{S^*}{E^*}\frac{1}{S^*}\left(1-\frac{S^*}{S}\right)S'+\frac{V^*}{E^*V^*}\left(1-\frac{V^*}{V}\right)V'+\frac{1}{E^*}\left(1-\frac{E^*}{E}\right)E'\\&+\frac{(\beta_1 I^*+\beta_2 D^*+\beta_3 H^*)(S^*+V^*\eta)I^*}{\sigma(E^*)^2}\frac{1}{I^*}\left(1-\frac{I^*}{I}\right)I'\\&+\frac{\beta_3(S^*+V^*\eta)(H^*)^2}{\phi E^*I^*}\frac{1}{H^*}\left(1-\frac{H^*}{H}\right)H'+\frac{\beta_2(V^*\eta+S^*)(D^*)^2}{\gamma\delta E^*I^*}\frac{1}{D^*}\left(1-\frac{D^*}{D}\right)D'.\end{aligned}$$

Continuing with the derivation, we express it as

$$\begin{aligned}U'(t)=&\frac{S^*}{E^*}\frac{1}{S^*}\left(1-\frac{S^*}{S}\right)((\beta_1 I^*+\beta_2 D^*+\beta_3 H^*)S^*+\mu S^*-(\beta_1 I+\beta_2 D+\beta_3 H)S-\mu S)\\&+\frac{V^*}{E^*}\frac{1}{V^2}\left(1-\frac{V^*}{V}\right)(\eta(\beta_1 I^*+\beta_2 D^*+\beta_3 H^*)V^*+\mu V^*-\eta(\beta_1 I+\beta_2 D+\beta_3 H)V-\mu V)\\&+\frac{1}{E^*}\left(1-\frac{E^*}{E}\right)\left((\beta_1 I+\beta_2 D+\beta_3 H)(S+\eta V)-\frac{(\beta_1 I^*+\beta_2 D^*+\beta_3 H^*)(S^*+\eta V^*)E}{E^*}\right)\\&+\frac{(\beta_1 I^*+\beta_2 D^*+\beta_3 H^*)(S^*+\eta V^*)I^*}{\sigma(E^*)^2}\frac{1}{I^*}\left(1-\frac{I^*}{I}\right)\left(\sigma E-\frac{\sigma E^*I}{I^*}\right)\\&+\frac{\beta_3(S^*+V^*)(H^*)^2}{\phi E^*I^*}\frac{1}{H^*}\left(1-\frac{H^*}{H}\right)\left(\phi I-\frac{\phi I^*H}{H^*}\right)\\&+\frac{B_2(S^*+V^*)(D^*)^2}{\delta\gamma_1 I^*E^*}\frac{1}{D^*}\left(1-\frac{D^*}{D}\right)\left(\delta\gamma_1 I-\frac{\delta\gamma_1 I^*D}{D^*}\right),\end{aligned}$$

$$\begin{aligned}U'(t)\leq&\frac{\beta_1 I^*S^*}{E^*}\left(1-\frac{S^*}{S}-\frac{IS}{I^*S^*}+\frac{I}{I^*}\right)+\frac{\beta_2 D^*S^*}{E^*}\left(1-\frac{S^*}{S}-\frac{SD}{S^*D^*}+\frac{D}{D^*}\right)\\&+\frac{\beta_3 H^*S^*}{E^*}\left(1-\frac{S^*}{S}-\frac{HS}{H^*S^*}+\frac{H}{H^*}\right)+\frac{\eta\beta_1 I^*V^*}{E^*}\left(1-\frac{V^*}{V}-\frac{IV}{I^*V^*}+\frac{I}{I^*}\right)\\&+\frac{\eta\beta_2 D^*V^*}{E^*}\left(1-\frac{V^*}{V}-\frac{DV}{D^*V^*}+\frac{D}{D^*}\right)+\frac{\eta\beta_3 H^*V^*}{E^*}\left(1-\frac{V^*}{V}-\frac{HV}{H^*V^*}+\frac{H}{H^*}\right)\\&+\frac{\beta_1 I^*S^*}{E^*}\left(\frac{IS}{I^*S^*}-\frac{E^*SI}{ES^*I^*}-\frac{E}{E^*}+1\right)+\frac{\beta_2 S^*D^*}{E^*}\left(\frac{SD}{S^*D^*}-\frac{E^*SD}{ES^*D^*}-\frac{E}{E^*}+1\right)\\&+\frac{\beta_3 H^*S^*}{E^*}\left(\frac{HS}{H^*S^*}-\frac{E^*HS}{EH^*S^*}-\frac{E}{E^*}+1\right)+\frac{\eta\beta_1 I^*V^*}{E^*}\left(\frac{IV}{I^*V^*}-\frac{E^*VI}{EV^*I^*}-\frac{E}{E^*}+1\right)\\&+\frac{\eta\beta_2 D^*V^*}{E^*}\left(\frac{DV}{D^*V^*}-\frac{E^*DV}{ED^*V^*}-\frac{E}{E^*}+1\right)+\frac{\eta\beta_3 H^*V^*}{E^*}\left(\frac{HV}{H^*V^*}-\frac{E^*HV}{EH^*V^*}-\frac{E}{E^*}+1\right)\\&+\frac{(\beta_1 I^*+\beta_2 D^*+\beta_3 H^*)(S^*+\eta V^*)}{E^*}\left(\frac{E}{E^*}-\frac{I^*E}{IE^*}-\frac{I}{I^*}+1\right)\\&+\frac{\beta_3(S^*+\eta V^*)H^*}{E^*}\left(\frac{I}{I^*}-\frac{IH^*}{I^*H}-\frac{H}{H^*}+1\right)+\frac{\beta_2(S^*+\eta V^*)D^*}{E^*}\left(\frac{I}{I^*}-\frac{ID^*}{I^*D}-\frac{D}{D^*}+1\right),\end{aligned}$$

$$
\begin{aligned}
U'(t) \leq & \frac{\beta_1 I^* S^*}{E^*}\left(\frac{I}{I^*}-\ln\frac{I}{I^*}-\frac{IS}{I^*S^*}+\ln\frac{IS}{I^*S^*}\right)+\frac{\beta_2 S^* D^*}{E^*}\left(-\ln\frac{D}{D^*}-\frac{DS}{D^*S^*}+\frac{D}{D^*}+\ln\frac{DS}{D^*S^*}\right)\\
& +\frac{\beta_3 H^* S^*}{E^*}\left(\frac{H}{H^*}-\ln\frac{H}{H^*}-\frac{HS}{H^*S^*}+\ln\frac{HS}{H^*S^*}\right)+\frac{\eta\beta_1 V^* I^*}{E^*}\left(\frac{I}{I^*}-\ln\frac{I}{I^*}-\frac{IV}{I^*V^*}+\ln\frac{IV}{I^*V^*}\right)\\
& +\frac{\eta\beta_2 D^* V^*}{E^*}\left(\frac{D}{D^*}-\ln\frac{D}{D^*}-\frac{DV}{D^*V^*}+\ln\frac{DV}{D^*V^*}\right)+\frac{\eta\beta_3 H^* V^*}{E^*}\left(\frac{H}{H^*}-\ln\frac{H}{H^*}-\frac{HV}{H^*V^*}+\ln\frac{HV}{H^*V^*}\right)\\
& +\frac{\beta_1 I^* S^*}{E^*}\left(\frac{IS}{I^*S^*}-\ln\frac{IS}{I^*S^*}-\frac{E}{E^*}+\ln\frac{E}{E^*}\right)+\frac{\beta_2 D^* S^*}{E^*}\left(\frac{DS}{D^*S^*}-\ln\frac{DS}{D^*S^*}-\frac{E}{E^*}+\ln\frac{E}{E^*}\right)\\
& +\frac{\beta_3 H^* S^*}{E^*}\left(\frac{HS}{H^*S^*}-\ln\frac{HS}{H^*S^*}-\frac{E}{E^*}+\ln\frac{E}{E^*}\right)+\frac{\eta\beta_1 V^* I^*}{E^*}\left(\frac{IV}{I^*V^*}-\ln\frac{IV}{I^*V^*}-\frac{E}{E^*}+\ln\frac{E}{E^*}\right)\\
& +\frac{\eta\beta_2 D^* V^*}{E^*}\left(\frac{DV}{D^*V^*}-\ln\frac{DV}{D^*V^*}-\frac{E}{E^*}+\ln\frac{E}{E^*}\right)+\frac{\eta\beta_3 H^* V^*}{E^*}\left(\frac{HV}{H^*V^*}-\ln\frac{HV}{H^*V^*}-\frac{E}{E^*}+\ln\frac{E}{E^*}\right)\\
& +\frac{(\beta_1 I^*+\beta_2 D^*+\beta_3 H^*)(S^*+\eta V^*)}{E^*}\left(\frac{E}{E^*}-\ln\frac{E}{E^*}-\frac{I}{I^*}+\ln\frac{I}{I^*}\right)\\
& +\frac{\beta_2(S^*+\eta V^*)D^*}{E^*}\left(\frac{I}{I^*}-\ln\frac{I}{I^*}-\frac{D}{D^*}+\ln\frac{D}{D^*}\right)+\frac{\beta_3(S^*+\eta V^*)H^*}{E^*}\left(\frac{I}{I^*}-\ln\frac{I}{I^*}-\frac{H}{H^*}+\ln\frac{H}{H^*}\right),
\end{aligned}
$$

$$
\begin{aligned}
U'(t) = & \frac{\beta_1 I^*(S^*+\eta V^*)}{E^*}\left(\frac{I}{I^*}-\ln\frac{I}{I^*}-\frac{E}{E^*}+\ln\frac{E}{E^*}\right)\\
& +\frac{\beta_2 D^*(S^*+\eta V^*)}{E^*}\left(-\frac{E}{E^*}+\ln\frac{E}{E^*}\right)+\frac{\beta_3 H^*(S^*+\eta V^*)}{E^*}\left(-\frac{E}{E^*}+\ln\frac{E}{E^*}\right)\\
& \frac{(\beta_1 I^*+\beta_2 D^*+\beta_3 H^*)\,(S^*+\eta V^*)}{E^*}\left(\frac{E}{E^*}-\ln\frac{E}{E^*}-\frac{I}{I^*}+\ln\frac{I}{I^*}\right)+\frac{\beta_3 H^*(S^*+\eta V^*)}{E^*}\left(\frac{I}{I^*}-\ln\frac{I}{I^*}\right)\\
& +\frac{\beta_2(S^*+\eta V^*)D^*}{E^*}\left(\frac{I}{I^*}-\ln\frac{I}{I^*}\right),
\end{aligned}
$$

$$
U'(t) = 0. \tag{18}
$$

Since it is known that the time derivative of the Lyapunov function $U(t)$ is negative and equals zero only when the system variables satisfy $S = S^*, V = V^*, E = E^*, I = I^*, D = D^*, H = H^*$, the EE E_1 is the only positively invariant set within the feasible region Γ. LaSalle Invariance Principle states that all solutions to the system with initial states within the feasible region Γ converge to E_1 as $t \to \infty$. The EE E_1 is therefore global asymptotical stable whenever $R_0 > 1$.

□

5 Parameter estimation

Parameter estimation is a fundamental component in the modeling of epidemic dynamics, as it connects theoretical frameworks with real world data. By calibrating the model to observed data, it ensures that the mathematical structure accurately reflects the actual progression of an infectious disease over time. This process involves determining the optimal values for key parameters such as transmission rate, recovery rate, incubation period, isolation rate, and mortality rate that collectively govern the epidemic's dynamics.

Accurate parameter estimation enhances the model reliability and allows for the identification of critical thresholds like the basic reproduction number R_0, which is essential for designing effective public health strategies. Moreover, it enables the

forecasting of epidemic trends and the evaluation of potential interventions, such as vaccination campaigns, travel restrictions, or quarantine measures.

This section outlines the procedure used to estimate the parameters for the proposed epidemic model based on the actual 2015 Ebola outbreak data in Sierra Leone. According to [25], the incubation period of the Ebola virus is approximately 1.498. The average life expectancy in Sierra Leone is 60.41 years, which gives a weekly natural mortality rate μ calculated as

$$\mu = \frac{1}{\text{average life span} \times 52.14\,\text{weeks}} = \frac{1}{60.41 \times 52.14}.$$

The remaining parameters are estimated using the *Least Squares Method*, which fits the proposed model to the confirmed Ebola infection cases reported in Sierra Leone in 2015 outreak [25].

The cost function used in the parameter estimation procedure is defined as:

$$\Phi(\theta) = \sum_{i=1}^{n} r_i^2, \quad \text{where } r_i = y(t_i, \theta) - \bar{y}(t_i). \tag{19}$$

In Eq. (1), $y(t_i, \theta)$ represents the solution of the proposed model at time t_i using parameters θ, while $\bar{y}(t_i)$ denotes the corresponding reported data at time t_i. The term r_i is the residual, capturing the difference between the model prediction and the observed data. The total number of data points is denoted by n.

The objective is to minimize the sum of squares of resulting residuals $\Phi(\theta)$ to ensure the model's predictions closely match the real data. This optimization is implemented in Matlab and Python using the `least_squares` function from the `scipy.optimize` module. The `least_squares` function uses the residuals r_i, initial estimates of the parameters θ, and the Trust Region Reflective algorithm to find the optimal values.

The initial value for the susceptible population is set as $S(0) = 8791000$, based on [25], and the initial number of infections is $I(0) = 1$, taken from the reported 2015 data for the Sierra Leone region. The initial number of exposed individuals is assumed to be $E(0) = 50$. At the outbreak start, there were no vaccinated, hospitalized, recovered, or deceased individuals due to infection; hence, $V(0) = H(0) = R(0) = D(0) = 0$. Based on this optimization procedure, the optimal parameter values are obtained and summarized in Table 2. These values ensure the model predictions closely align with real world data, as illustrated in Fig. 2.

5.1 Numerical simulation

By adjusting one parameter at a time while maintaining the others at their estimated baseline values (as shown in Table 2), we conducted a sensitivity analysis to examine the effects of various parameters on the transmission dynamics of the Ebola virus. Changes in the behavior of the model were documented and visualized by slightly altering each parameter from its fitted value.

Table 2 Parameter descriptions and estimated values

Parameters	Physical meaning	Value [per week]	Source
Λ	Recruitment rate	2790	Estimated
μ	Death rate	3.1511774×10^{-3}	Estimated
ρ	Proportion of vaccinated individuals	9.98279×10^{-1}	Fitting from data
β_1	Transmission rate from $I(t)$	9.97476×10^{-1}	Fitting from data
β_2	Transmission rate from $D(t)$	6.99541×10^{-1}	Fitting from data
β_3	Transmission rate from $H(t)$	9.99156×10^{-2}	Fitting from data
η	Efficacy of vaccination	9.98737×10^{-1}	Fitting from data
ϕ	Rate from infectious to hospitalized	9.88437×10^{-1}	Fitting from data
γ_1	Recovery rate from infection	8.43319×10^{-1}	Fitting from data
γ_2	Recovery rate from hospitalization	8.37717×10^{-2}	Fitting from data
δ	Fraction of lethal cases	3.55149×10^{-1}	Fitting from data
α	Rate of burial	1.04738×10^{-1}	Fitting from data

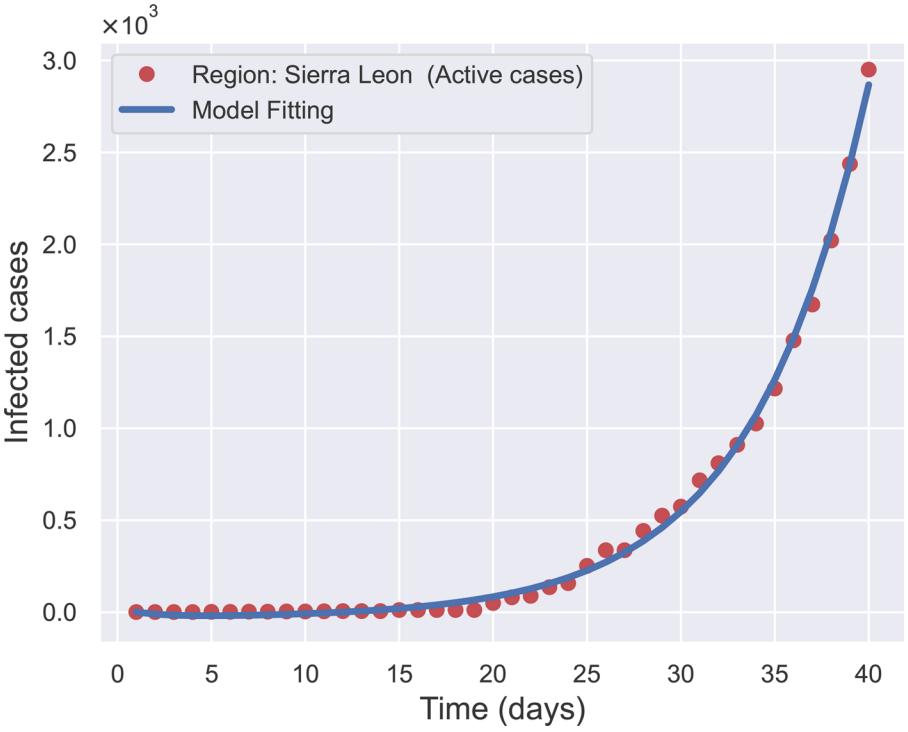

Fig. 2 Model fitting based on real data of the Ebola outbreak in Sierra Leone (2015)

The impact of changing the human-to-human transmission rate, β_1 is depicted in Fig. 3. A greater peak and a quicker epidemic are the results of the illness spreading more quickly among susceptible people as β_1 rises. Reduced infection burden and slower disease progression are the results of a decrease in β_1.

The impact of β_2, denoting the rate of transmission from deceased persons to vulnerable humans is shown in Fig. 4. These plots show that an increase in β_2 raises the number of infections, highlighting the significance of safe and quick burial procedures.

The effect of β_3, that is the transmission rate from hospitalized individuals is the main focus of Fig. 5. Given that this value is so low, even small adjustments have noticeable but insignificant effects on the dynamics of the disease, suggesting that infection control in hospitals can greatly lower secondary transmission.

Figure 6 examines shifts in ϕ, the hospitalization rate of infected people. Higher hospitalization rates result in faster isolation of contagious individuals, which lowers overall infection rates and improves epidemic management.

Figure 7 examines the effects of variations in γ_2, the hospitalization recovery rate, on the model. A lower value of γ_2 delays recovery, which may increase the burden of disease, whereas a higher value shortens hospital stay durations, which may reduce hospital overcrowding.

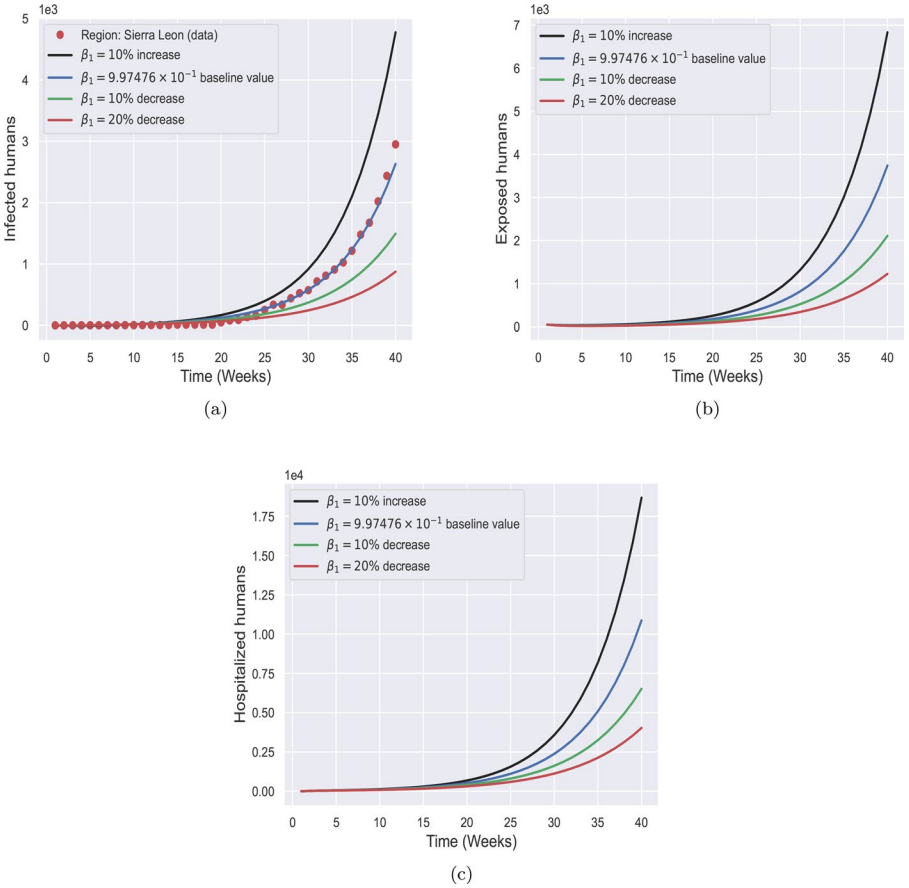

Fig. 3 Simulation output illustrating how changes in β_1 affect model predictions, using 9.97476×10^{-1} as the baseline value

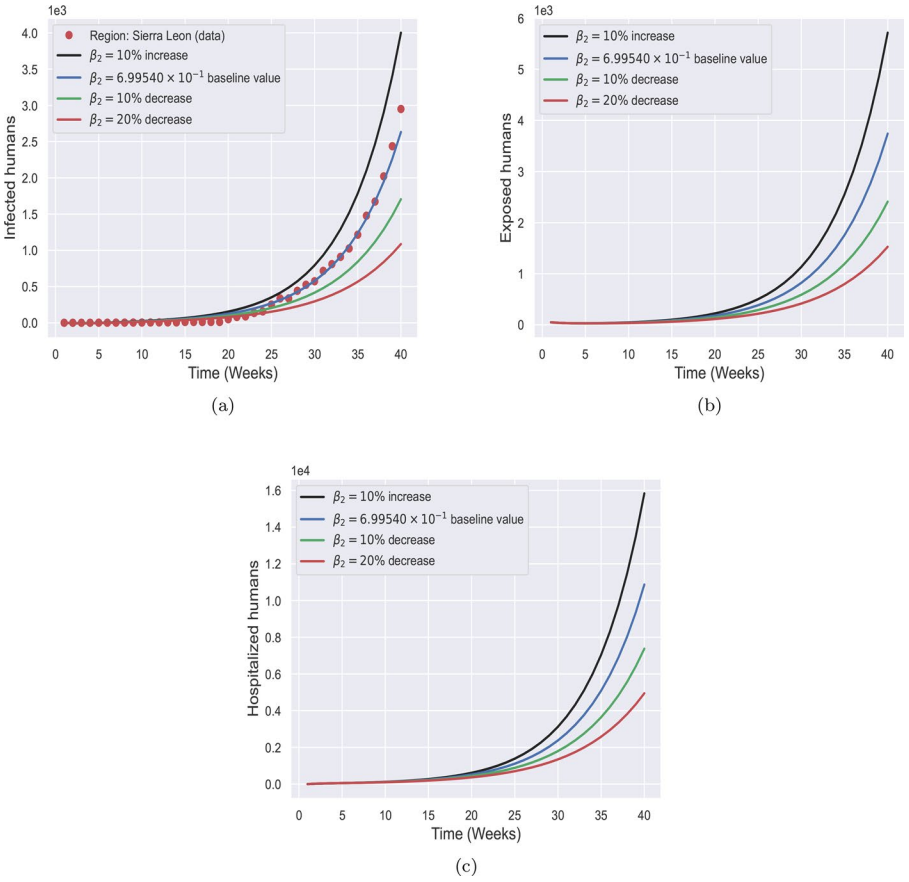

Fig. 4 Simulation results showing the impact of varying β_2 values compared to the baseline 6.99541×10^{-1}

The impact of δ, the percentage of fatal cases, is examined in Fig. 8. In addition to decreasing the size of the infected population, a higher δ raises the number of deaths, which indirectly influences the dynamics of disease transmission through deceased related contacts (linked to β_2).

The burial rate α is examined in Fig. 9. Faster and safely burial (higher α) reduces the number of new infections by limiting the spread of disease from deceased people. On the other hand, delayed burials (lower α) increase the risk of exposure and exacerbate the spread of disease.

6 Sensitivity analysis

Sensitivity analysis is an essential aspect of epidemic modeling as it enables the evaluation of how variations in model parameters influence the overall model behavior. Specifically, it helps in evaluating the sensitivity of the basic reproduction number

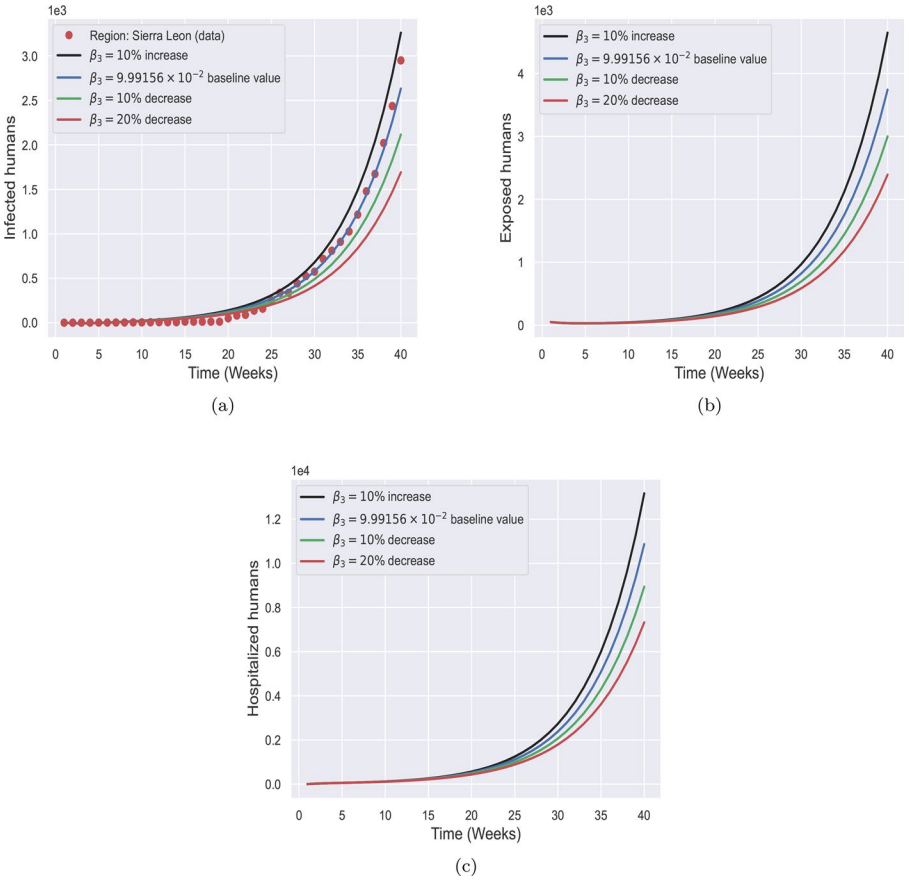

Fig. 5 Simulation outcomes for varying values of β_3, referenced against the baseline value 9.99156×10^{-2}

R_0, a crucial threshold parameter that indicates whether an infectious disease is likely to spread or die out within a population. Following the methodology outlined in [33], the primary goal of the sensitivity analysis presented here is to identify the parameters that most significantly impact on R_0. Parameters exhibiting a positive sensitivity index have a direct relationship with R_0, indicating that an increase in such parameters will result in a higher value of R_0. Conversely, parameters with negative indices are inversely related to R_0, suggesting that reducing these parameters can contribute to decreasing the spread of the disease. To quantify the impact of each parameter on R_0, normalized forward sensitivity indices are computed using the following formula:

$$S_{\zeta}^{R_0} = \frac{\zeta}{R_0} \cdot \frac{\partial R_0}{\partial \zeta}, \tag{20}$$

where ζ represents a parameter of the model. Utilizing Eq. (20), numerical value for each sensitivity index are derived in Table 3, with a graphical representation shown in

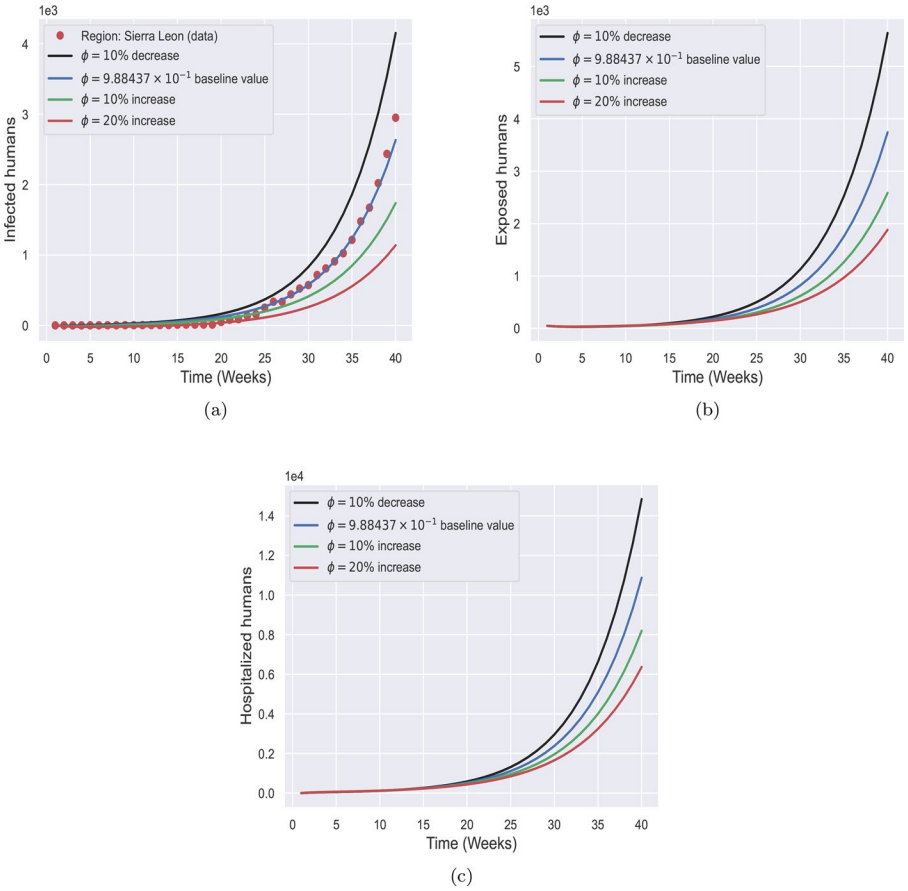

Fig. 6 Simulation results corresponding to different values of ϕ, with reference to the baseline value 9.88437×10^{-1}

Fig. 10. The sensitivity analysis presented in Fig. 10 illustrates the relative influence of model parameters on the basic reproduction number R_0. Parameters β_1, β_2, β_3, and δ show the considerable positive sensitivity indices, indicating that enhancement in these parameters notionally increase R_0, thereby intensifying disease transmission. Conversely, parameters such as ϕ, γ_2, and α exhibit negative sensitivity indices, suggesting that strengthening these processes contributes to reduce R_0. The relatively small indices of ρ and η highlight their limited impact on disease dynamics.

7 Optimization of Ebola model

One of the primary objectives of both public health and mathematical epidemiology is to understand how to prevent, control, and ultimately eradicate infectious diseases [34]. Optimal control theory serves as an effective tool for designing intervention strategies that support disease eradication and minimize the overall burden of infec-

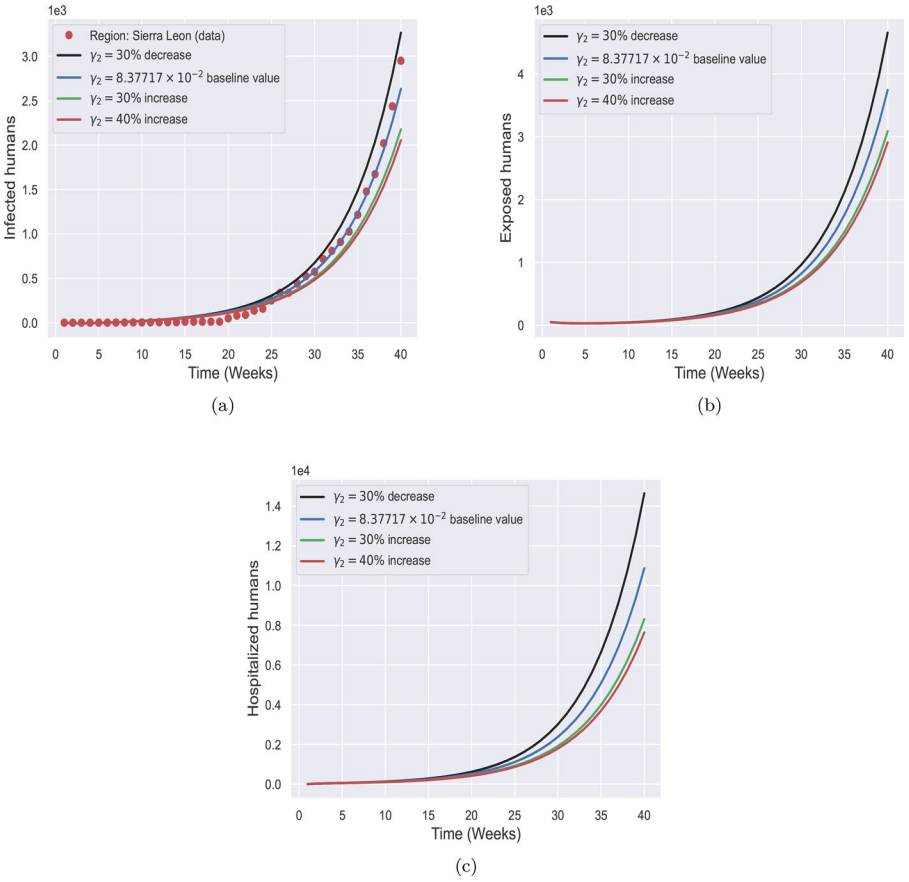

Fig. 7 Simulation outcomes for varying values of γ_2, using the baseline value 9.99541×10^{-1} for comparison

tion. To incorporate intervention strategies against the spread of EVD, we introduce three time dependent control variables denoted by $u_1(t)$, $u_2(t)$, and $u_3(t)$. These controls are chosen based on sensitivity analysis and defined as follows.

- $u_1(t)$: **Protective measures for the susceptible and vaccinated individuals**
  This control represents implementation protective measures for the susceptible and vaccinated individuals. Such measures may include public education campaigns, use of personal protective equipment, restriction of movement, and avoidance of contact with infectious individuals or contaminated environments.
- $u_2(t)$: **Measures to enhance secure burial of deceased individuals**
  This control accounts for the measure to enhance safe burial of deceased individuals who died from Ebola. These measures also include efforts to shorten the average time length until burial of deceased individual.

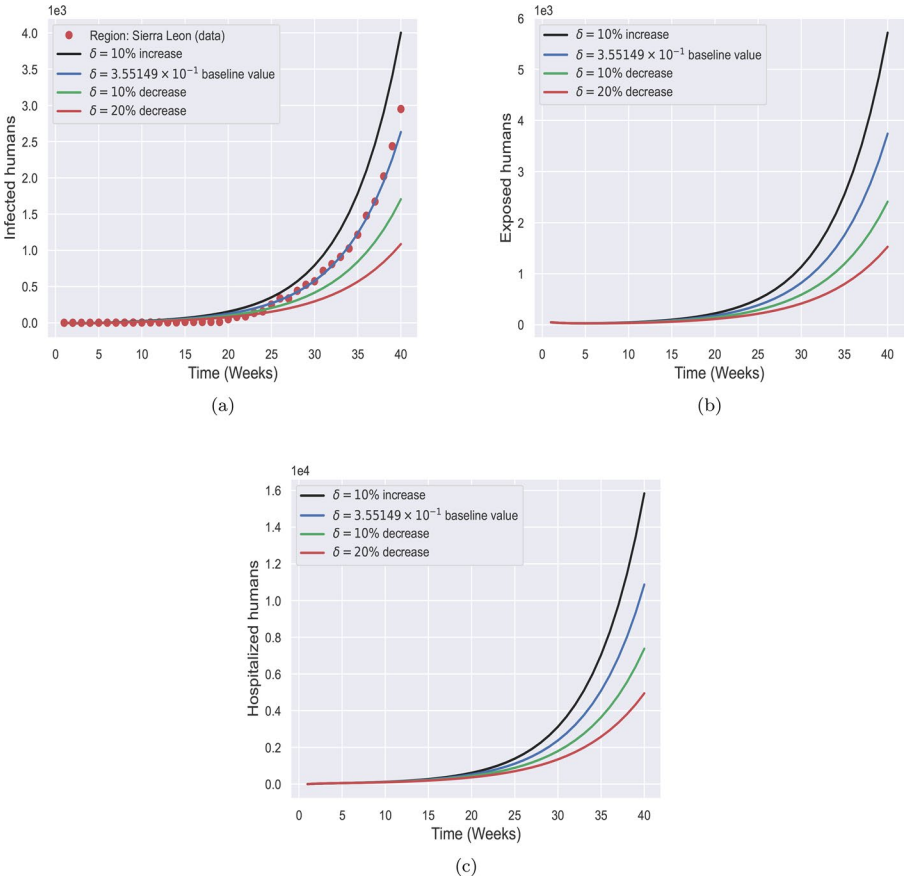

Fig. 8 Simulation results corresponding to varying values of δ, compared to the baseline value of 3.5514×10^{-1}

- $u_3(t)$: **Measures to enhance hospitalization of infected individuals**
  This variable denotes the timely and effective treatment/hospitalization rate of infected individuals.

These control functions are thought to be Lebesgue measurable and have a [0,1] bound. In order to minimize an objective functional that strikes a balance between the cost of intervention and the health impact of the epidemic, their ideal time profiles are determined using Pontryagin Maximum Principle. This framework makes it possible to identify effective and realistic methods for controlling epidemics when resources are limited. Implementing the above control variables, the following controlled model is obtained

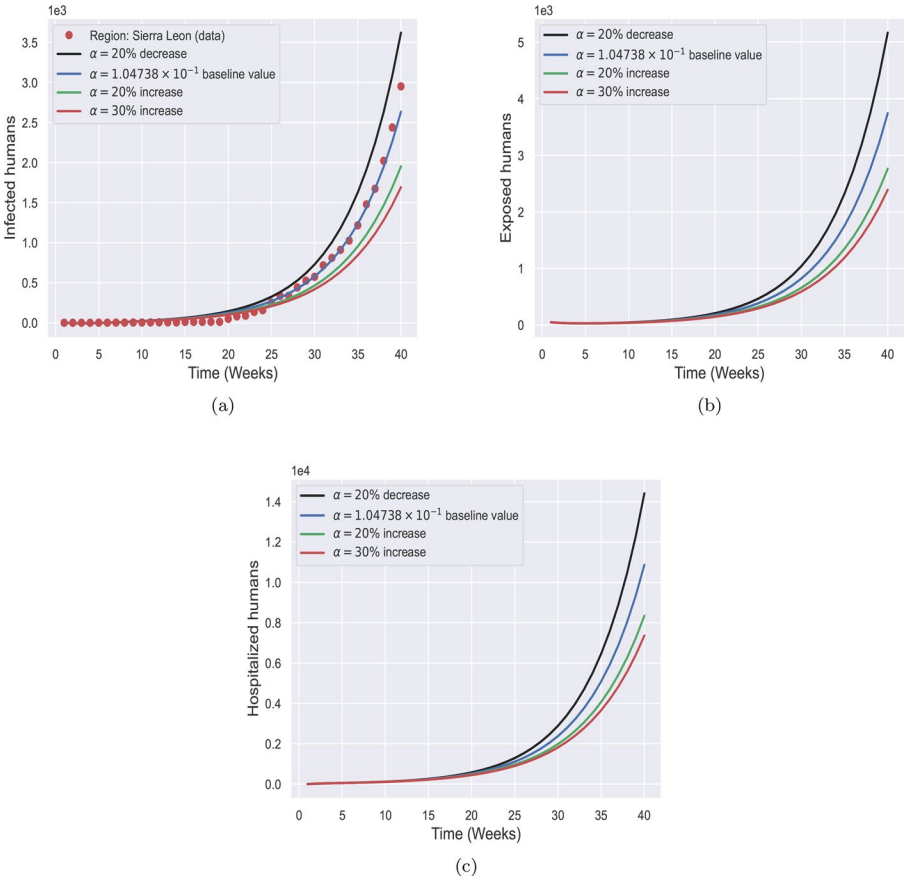

Fig. 9 Model output under varying values of α, compared with the baseline value of 1.04738×10^{-1}

Table 3 Model parameters sensitivity indices

Parameter	Sensitivity Index
ρ	0.001260
β_1	0.24324
β_2	0.47231
β_3	0.28534
η	0.00171
ϕ	−0.25417
γ_2	−0.28426
δ	0.47231
α	−0.47231

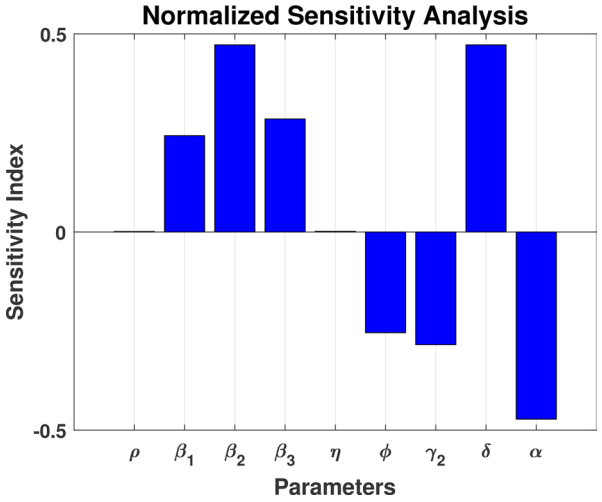

Fig. 10 Sensitivity indices of the model parameters on the basic reproduction number R_0

$$\begin{cases} S'(t) &= \rho\Lambda - \frac{(\beta_1 I+\beta_2 D+\beta_3 H)S(1-u_1)}{N} - \mu S, \\ V'(t) &= (1-\rho)\Lambda - \frac{\eta(\beta_1 I+\beta_2 D+\beta_3 H)V(1-u_1)}{N} - \mu V, \\ E'(t) &= \frac{(\beta_1 I+\beta_2 D+\beta_3 H)S(1-u_1)}{N} + \frac{(\beta_1 I+\beta_2 D+\beta_3 H)\eta V(1-u_1)}{N} - (\mu+\sigma)E(t), \\ I'(t) &= \sigma E(t) - u_3 I(t) - (\gamma_1+\mu)I(t), \\ H'(t) &= u_3 I(t) - (\gamma_2+\mu)H(t), \\ R'(t) &= (1-\delta)\gamma_1 I(t) + \gamma_2 H(t) - \mu R(t), \\ D'(t) &= \gamma_1\delta I(t) - u_2 D(t), \end{cases} \tag{21}$$

subject to nonnegative initial values of state variables. The aim is to reduce both the burden of the infection and the cost associated with implementing control measures. The objective functional is given by

$$\begin{aligned} J(u_1,u_2,u_3) = \int_0^{T_f} & (A_1E(t) + A_2I(t) + A_3H(t) + A_4D(t) \\ & + \frac{1}{2}(A_5u_1^2(t) + A_6u_2^2(t) + A_7u_3^2(t)))dt, \end{aligned} \tag{22}$$

where the constants A_i, for $i = 1, 2, \ldots, 7$, represent weight parameters for the state and control variables, and T_f is the final time. The objective is to find optimal controls $u_1^*(t), u_2^*(t), u_3^*(t)$ such that:

$$J(u_1^*, u_2^*, u_3^*) = \min_{(u_1,u_2,u_3)\in\Omega} J(u_1,u_2,u_3), \tag{23}$$

with the admissible control set defined as:

$$\Omega = \{(u_1,u_2,u_3) : [0,T_f] \to [0,1] \,|\, u_1,u_2,u_3 \text{ are Lebesgue measurable}\}. \tag{24}$$

The Lagrangian associated with this control problem is:

$$L = A_1E + A_2I + A_3H + A_4D + \frac{1}{2}\left(A_5u_1^2 + A_6u_2^2 + A_7u_3^2\right). \tag{25}$$

Consequently, the Hamiltonian $\mathcal{H}$ relative to the optimal system is expressed as

$$\mathcal{H} = L + \lambda_1 S' + \lambda_2 V' + \lambda_3 E' + \lambda_4 I' + \lambda_5 H' + \lambda_6 R' + \lambda_7 D'. \tag{26}$$

Where $\lambda_i(t)$ are the adjoint variables corresponding to each state variable. The Hamiltonian $\mathcal{H}$ corresponding to the formulated optimal control problem is defined as follows

$$\begin{aligned}
\mathcal{H} =& A_1E + A_2I + A_3H + \frac{1}{2}\left(A_5u_1^2 + A_6u_2^2 + A_7u_3^2\right) \\
&+ \lambda_1\left(\rho\Lambda - \frac{(\beta_1 I + \beta_2 D + \beta_3 H)S(1-u_1)}{N} - \mu S\right) \\
&+ \lambda_2\left((1-\rho)\Lambda - \frac{\eta(\beta_1 I + \beta_2 D + \beta_3 H)V(1-u_1)}{N} - \mu V\right) \\
&+ \lambda_3\left(\frac{(\beta_1 I + \beta_2 D + \beta_3 H)(1-u_1)S}{N} + \frac{(\beta_1 I + \beta_2 D + \beta_3 H)(1-u_1)\eta V}{N} - (\sigma+\mu)E\right) \\
&+ \lambda_4\Big(\sigma E - u_3 I - (\gamma_1 + \mu)I\Big) \\
&+ \lambda_5\Big(u_3 I - (\gamma_2 + \mu)H\Big) \\
&+ \lambda_6\Big((1-\delta)\gamma_1 I + \gamma_2 H - \mu R\Big) \\
&+ \lambda_7\Big(\delta\gamma_1 I - u_2 D\Big).
\end{aligned} \tag{27}$$

Here, $\lambda_j(t)$ for $j = 1, \ldots, 7$ represent the adjoint variables.

7.1 Solution of the optimal control

By employing Pontryagin Maximum Principle, the following necessary conditions for optimality are derived.

$$\begin{cases}
\frac{dz}{dt} = -\frac{\partial \mathcal{H}(t,u_j^*,\lambda_j)}{\partial \lambda_j}, \\
\frac{\partial \mathcal{H}(t,u_j^*,\lambda_j)}{\partial u} = 0, \\
\frac{d\lambda_j(t)}{dt} = -\frac{\partial \mathcal{H}(t,u_j^*,\lambda_j)}{\partial z}.
\end{cases} \tag{28}$$

The adjoint system becomes

$$\frac{\partial \lambda_1}{\partial t} = \frac{(\beta_1 I + \beta_2 D + \beta_3 H)(N-S)(1-u_1)}{N^2}(\lambda_1 - \lambda_3) + \frac{\eta(\beta_1 I + \beta_2 D + \beta_3 H)V(1-u_1)}{N^2}(\lambda_3 - \lambda_1) + \mu\lambda_1.$$
$$\frac{\partial \lambda_2}{\partial t} = \frac{\eta(\beta_1 I + \beta_2 D + \beta_3 H)(N-V)(1-u_1)}{N^2}(\lambda_2 - \lambda_3) + \frac{(\beta_1 I + \beta_2 D + \beta_3 H)(1-u_1)S}{N^2}(\lambda_3 - \lambda_1) + \mu\lambda_2.$$
$$\frac{\partial \lambda_3}{\partial t} = -A_1 + \frac{(\beta_1 I + \beta_2 D + \beta_3 H)(1-u_1)}{N^2}\Big((S+\eta V)\lambda_3 - S\lambda_1 - \eta V\lambda_2\Big) + \lambda_3(\sigma + u_1) - \lambda_4\sigma.$$
$$\frac{\partial \lambda_4}{\partial t} = -A_2 + \frac{(1-u_1)}{N^2}(\beta_1 N - (\beta_1 I + \beta_2 D + \beta_3 H))\Big(\lambda_1 S + \lambda_2\eta V - \lambda_3(S+\eta V)\Big) + \lambda_4(u_3 + \gamma_1 + \mu)$$
$$- \lambda_5 u_3 + \lambda_6(1-\delta)\gamma_1 - \lambda_7\delta\gamma_1.$$
$$\frac{\partial \lambda_5}{\partial t} = -A_3 + \frac{\big(\beta_3 N - (\beta_1 I + \beta_2 D + \beta_3 H)(1-u_1)\big)}{N^2}\Big(\lambda_1 S + \lambda_2\eta V - \lambda_3(S+\eta V)\Big) + \lambda_5(\gamma_2 + \mu) - \lambda_6\gamma_2.$$
$$\frac{\partial \lambda_6}{\partial t} = \frac{(\beta_1 I + \beta_2 D + \beta_3 H)(1-u_1)}{N^2}\Big(\lambda_3(S+\eta V) - \lambda_1 S - \lambda_2\eta V\Big) + \lambda_6\mu.$$
$$\frac{\partial \lambda_7}{\partial t} = \frac{\big(\beta_2 N - (\beta_1 I + \beta_3 H + \beta_2 B\big)(1-u_1)}{N^2}(\lambda_1 S + \lambda_2\eta V - \lambda_3(S+\eta V)) + \lambda_7 u_2.$$

To derive the optimal control functions, the Hamiltonian is partially differentiated with respect to each control variable

$$\frac{\partial \mathcal{H}}{\partial u_1} = A_5 u_1 - \frac{\lambda_1(\beta_1 I + \beta_2 D + \beta_3 H)S}{N} + \frac{\lambda_3(\beta_1 I + \beta_2 D + \beta_3 H)S}{N}. \quad (29)$$

$$\frac{\partial \mathcal{H}}{\partial u_2} = A_6 u_2 + \frac{(\lambda_7 - \lambda_7)\eta(\beta_1 I + \beta_2 D + \beta_3 H)V}{N}. \quad (30)$$

$$\frac{\partial \mathcal{H}}{\partial u_3} = A_7 u_3 + (\lambda_5 - \lambda_4)I. \quad (31)$$

The optimal controls are obtain as follows

$$u_1^* = \frac{(\lambda_1 - \lambda_3)(\beta_1 I + \beta_2 D + \beta_3 H)S}{NA_5} + \frac{\eta(\beta_1 I + \beta_2 D + \beta_3 H)V(\lambda_3 - \lambda_2)}{NA_5}. \quad (32)$$

$$u_2^* = \frac{\lambda_7 D}{A_6}. \quad (33)$$

$$u_3^* = \frac{(\lambda_4 - \lambda_5)I}{A_7}. \quad (34)$$

8 Simulation of the control problem

The optimal control problem is designed to reduce the cost of implementing interventions and the disease burden over a predetermined period of time $T_f = 40$ weeks. We choose $A_1 = 5$, $A_2 = 0.01$, and $A_3 = 0.02$ for the simulation study. The constants $A_5 = 40$, $A_6 = 50$, and $A_7 = 30$ capture the cost of applying each control strategy and represent the weight of the control effort required for $u_1(t)$, $u_2(t)$, and $u_3(t)$, respectively. These values are assumed for the simulation and not based on experi-

mental study. We find control trajectories that strike a balance between minimizing infections and minimizing intervention costs by employing a 4th-order Runge-Kutta algorithm to solve this optimal control problem using the forward-backward sweep method. To investigate the efficacy of various control strategies. This section explains the impact of different combinations of control strategies, namely $u_1(t)$, $u_2(t)$, and $u_3(t)$, on the progression of the Ebola epidemic. Each control targets a specific population group: $u_1(t)$ aims to reduce exposure among susceptible individuals, $u_2(t)$ focuses on maintaining precautions among vaccinated individuals, and $u_3(t)$ represents the hospitalization and treatment of infectious individuals. The simulation outcomes for each case are analyzed below.

8.1 Scenario 1: triple controls implementation

All controls are implemented i.e., ($u_j \neq 0$, for $, j = 1, 2, 3$)

This case involves the simultaneous application of all three control measures. As illustrated in Fig. 11, the numbers of exposed, infected, and deceased individuals decrease significantly with the implementation of optimal controls, while the hospitalized and vaccinated populations increase over time. The implementation of optimal control measures reduces the incidence of infection, resulting in fewer individuals at risk and, consequently, fewer individuals recovering, as shown in Fig. 11(f). These results indicate that a combination of early prevention and prompt treatment effectively suppresses the outbreak. The initial high control effort, followed by a gradual reduction, reflects an optimal response strategy. This case clearly demonstrates that integrated interventions produce the most favorable outcome.

8.2 Scenario 2: couple controls implementation

Case 1: $u_j \neq 0$, for $, j = 2, 3$

In this scenario, we simulate the EVD model by implementing two control measures simultaneously. Case 1 considers the application of control measures u_2 and u_3, while the protective measure for susceptible and vaccinated individuals (denoted by u_1) is ignored. The simulations are presented in Fig. 12. It can be observed that with this set of controls, although the levels of exposure and infection remain low, they do not vanish over time. This indicates that implementing only u_2 and u_3 is not effective in fully curtailing the infection.

$Case2 : u_j \neq 0$, for $, j = 1, 3$

Case 2 considers the application of control measures u_1 and u_3, while the control u_2 is ignored. The resulting simulation is presented in Fig. 13. With this set of controls, although the trajectory of deceased individuals remains comparatively higher, the exposed and infected individuals vanish significantly over time. This indicates that implementing only u_1 and u_3 can contribute effectively to minimizing the infection.

$Case3 : u_j \neq 0$, for$, j = 1, 2$

This case excludes the time-dependent treatment control of infectious individuals u_3 but implements the prevention control measures u_1 and u_2. As shown in Fig. 14, in the absence of u_3, the infection is not suppressed immediately; instead, the exposed and infected populations decline more gradually and vanish over a comparatively

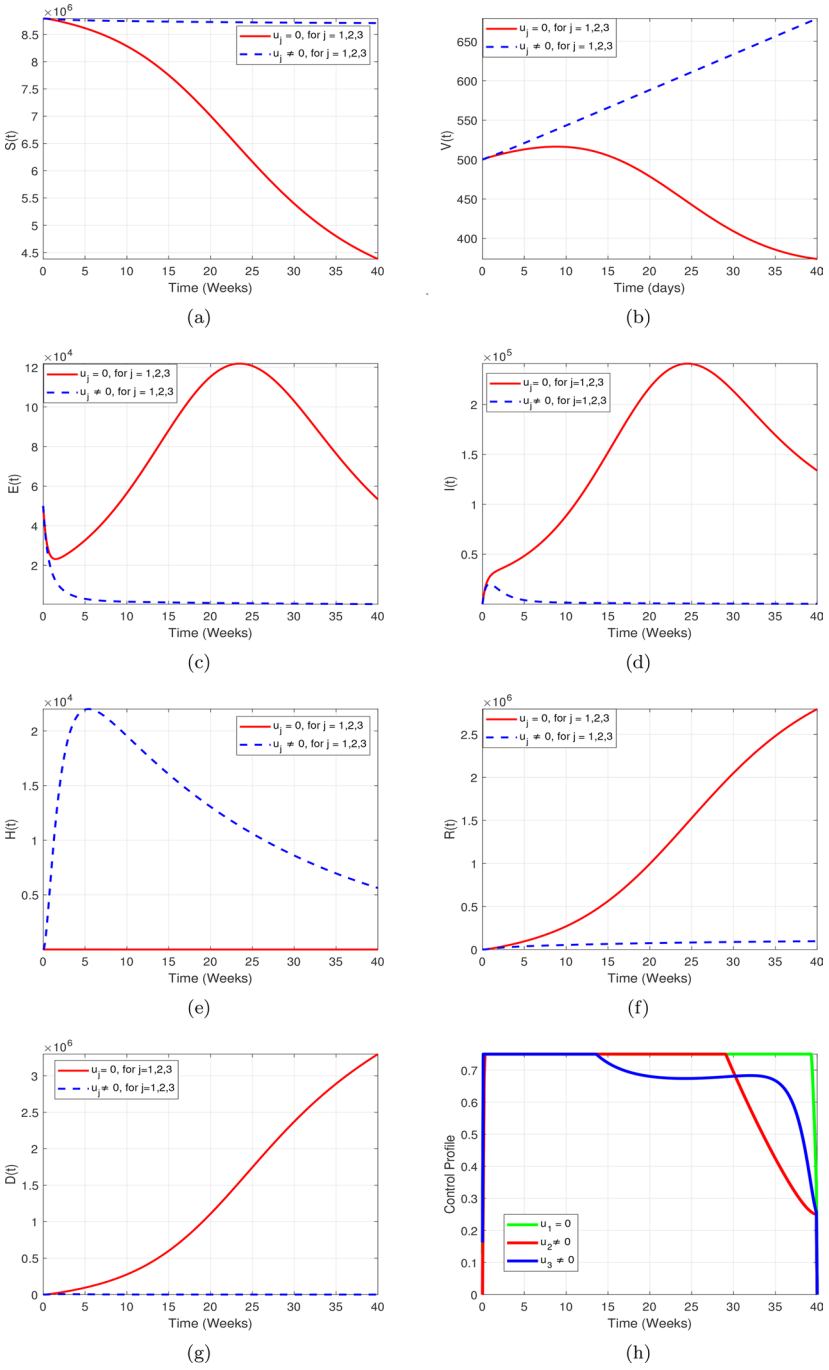

Fig. 11 Simulation results of the EVD model for scenario 1 when all control measures are active i.e., $u_j \neq 0$, for , $j = 1, 2, 3$

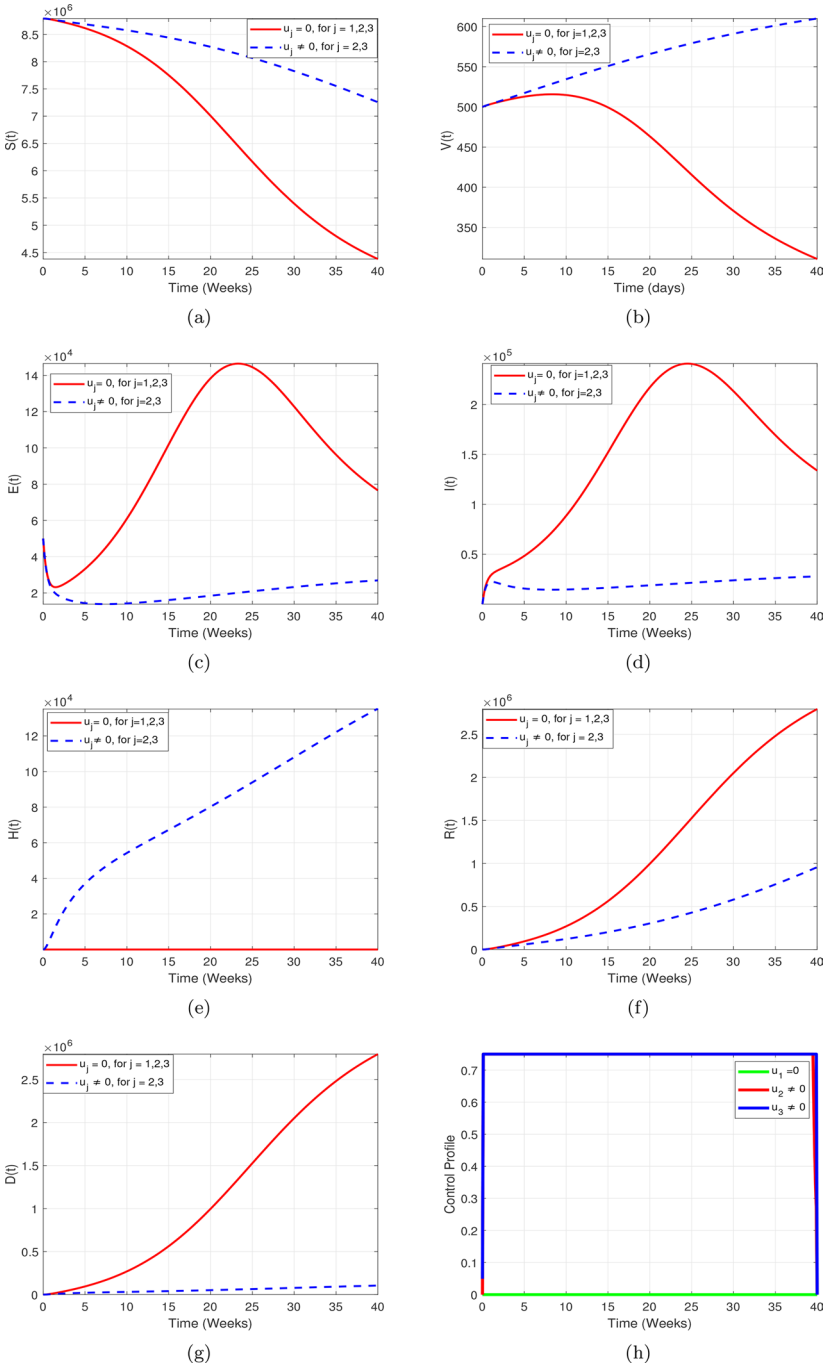

Fig. 12 Simulation results of the EVD model for the case 1 when $u_j \neq 0,$ for $, j = 2, 3$

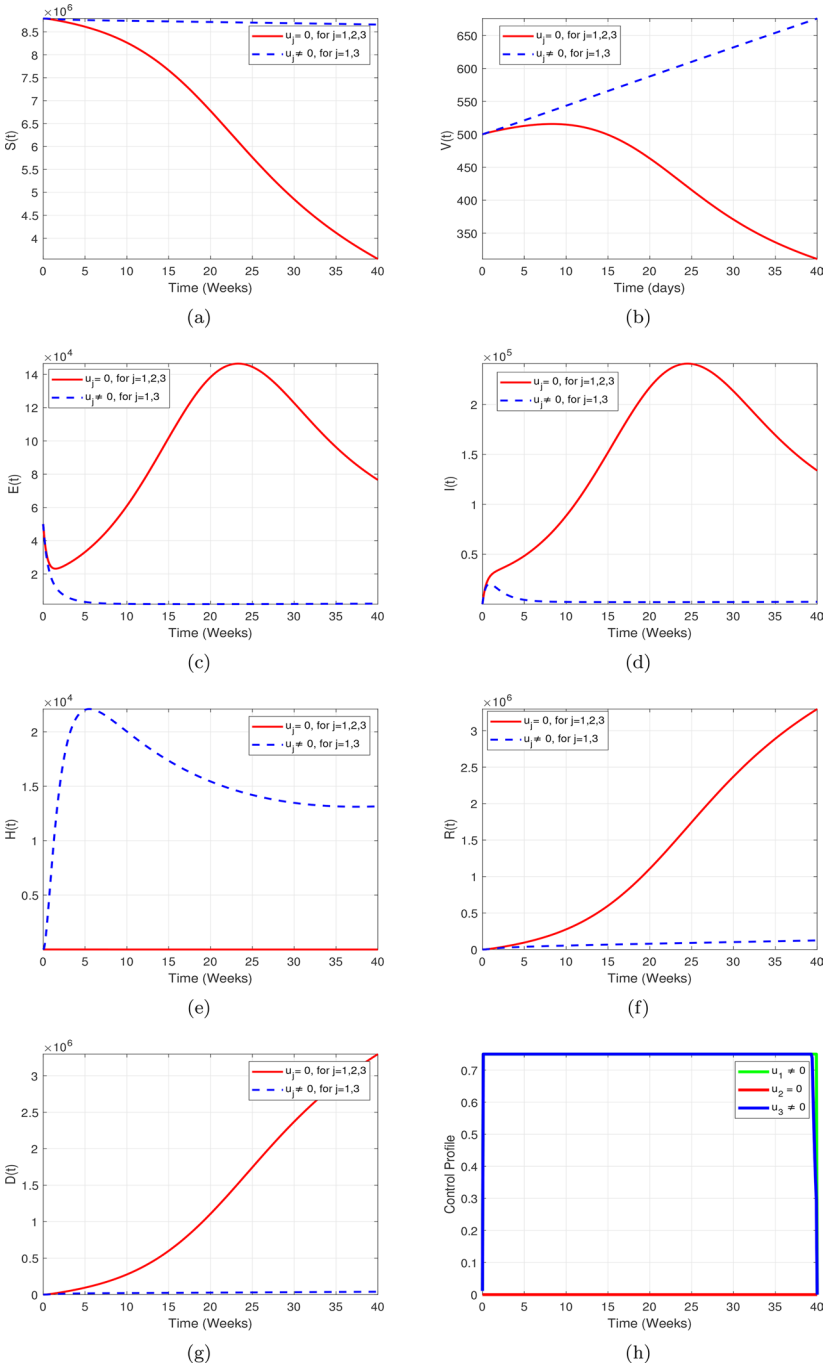

Fig. 13 Simulation results of the EVD model for the case 2 when $u_j \neq 0,$ for $, j = 1, 3$

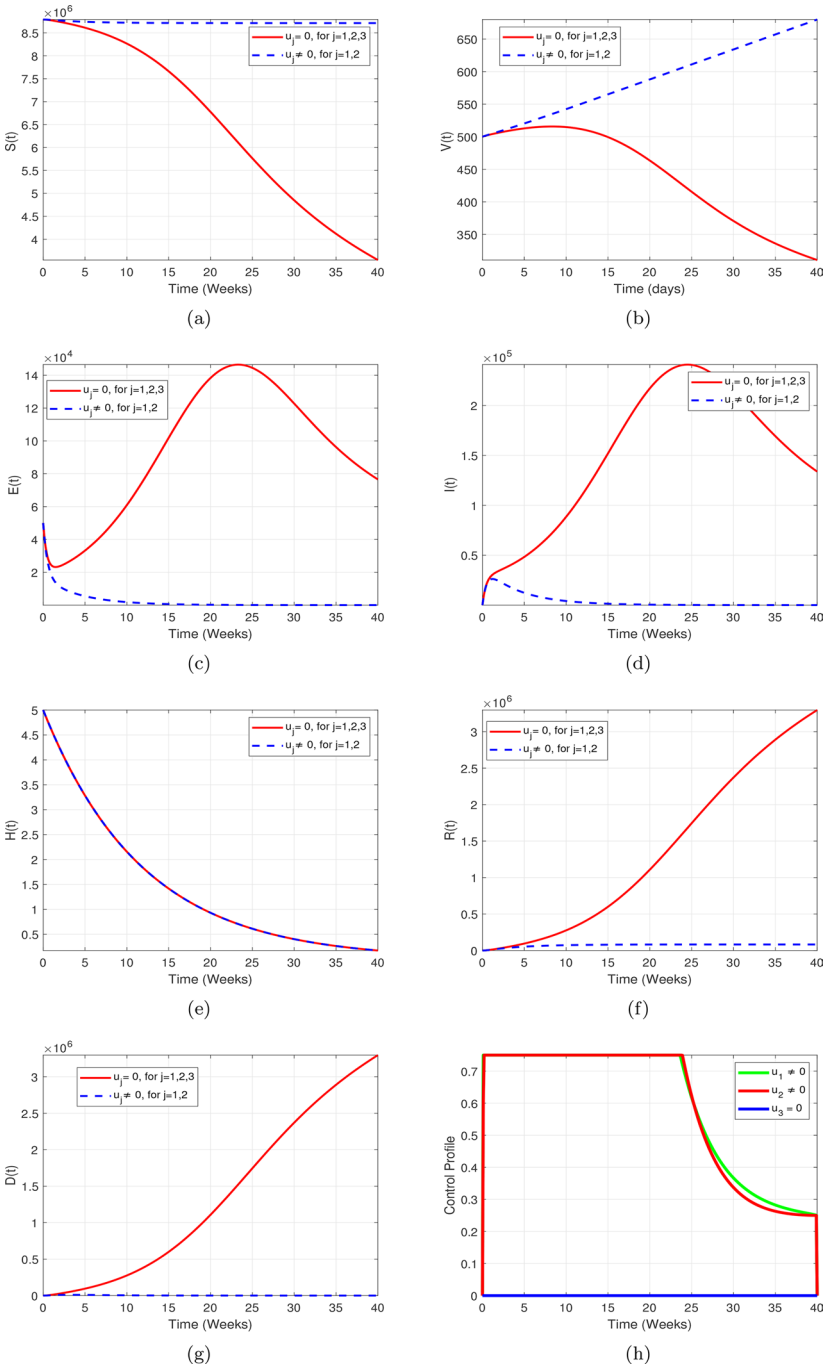

Fig. 14 Simulation results of the EVD model for the case 3 when $u_j \neq 0,$ for $, j = 1, 2$

longer time period. This outcome highlights that while prevention strategies (u_1 and u_2) are effective in reducing transmission by limiting new exposures, the absence of active treatment (u_3) slows down the clearance of existing infections. Therefore, although infection can eventually be eradicated, the time horizon required is longer compared to strategies that include treatment.

8.3 Scenario 3: single controls implementation

$u_j \neq 0$, for $, j = 3$

Scenario 3 considers the application of a single control variable, while the other two are not applied. We simulate the EVD model by activating only the treatment of infected individuals u_3. Figure 15 illustrates the simulation outcomes for all population groups under this control setting. It can be observed that this strategy fails to eradicate individuals in the exposed and infected classes. Thus, the results suggest that treatment alone is insufficient to effectively minimize the spread of the disease.

The comparison of all control scenarios confirms that a significant reduction in disease transmission is achieved when all control strategies are applied simultaneously. A coordinated and timely integration of preventive and therapeutic measures is therefore essential for effectively managing the spread of the EVD.

9 Conclusion

This research offers a comprehensive and data-driven analysis of an optimal control model for the spread of the Ebola virus, incorporating various transmission routes, including those from hospitalized and deceased individuals. The model is structured using a compartmental framework and extended to include the effects of hospitalization and vaccination interventions. Estimation of parameters with actual data from the 2015 Ebola outbreak in Sierra Leone enhances the model practical relevance and reliability. The optimal control problem is formulated with the goal of minimizing the total number of infections and deaths. Three time-dependent controls are introduced namely isolation or protective measures of susceptible and vaccinated individuals, effective treatment or hospitalization of infected individuals and to enhance safe and timely burial of infected deceased individuals. From a theoretical perspective, we derived conditions for the local and global stability of the disease-free and endemic equilibria. Specifically, the disease-free equilibrium is stable when the basic reproduction number $R_0 < 1$, while the endemic equilibrium becomes stable when $R_0 > 1$. Sensitivity analysis identifies the contact rate with deceased individuals and the efficiency of burial procedures as key factors influencing R_0, emphasizing the crucial role of safe and timely burials in reducing transmission. Simulation results highlight the comparative effectiveness of different control strategies in curtailing the infection burden. When all three interventions are implemented simultaneously, the epidemic is more effectively suppressed, resulting in a significant reduction in cumulative infections and fatalities. On the other hands, applying only one or two control strategies leads to delayed containment and higher peak infection levels. Among the control measures, continuous and high-intensity treatment of infected individuals emerges as

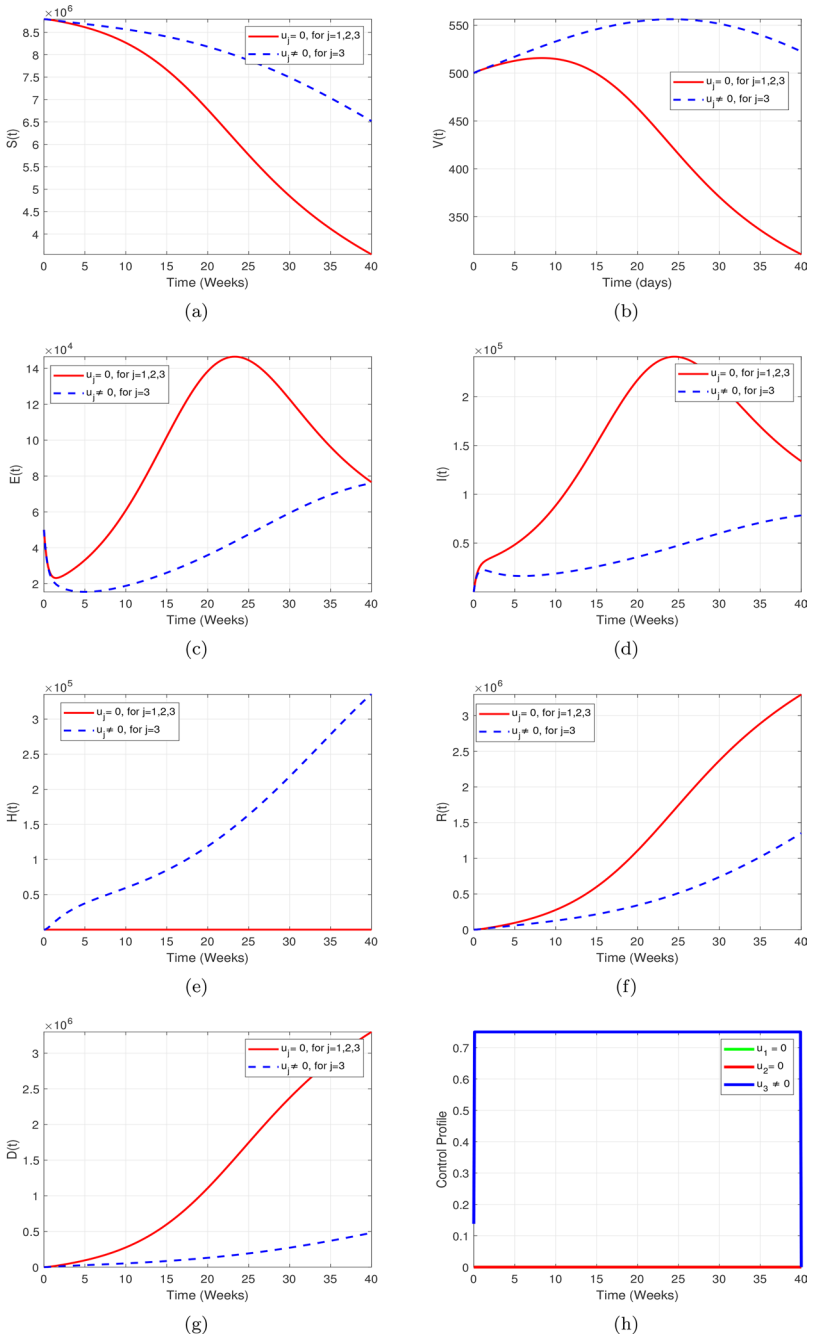

Fig. 15 Simulation results for the case 4 when $u_j \neq 0,$ for $, j = 3$

the most critical long-term intervention. We conclude that this study underscores the necessity of prompt, robust, and sustained interventions to effectively manage Ebola outbreaks. It also cautions against premature relaxation of control efforts. In future work, the model will be extended to incorporate vector-valued controls and to evaluate the combined impact of pharmaceutical and non-pharmaceutical interventions using fractional and stochastic epidemic modeling approaches. This advancement aims to support the development of more realistic data-driven public health policies for managing Ebola and other emerging infectious diseases.

Acknowledgements The authors are grateful to the reviewers for improving the quality of this work.

Author contributions All authors contributed equally.

Data availability This manuscript has no associated data.

Declarations

Competing Interests There are no competing interests regarding this work.

References

1. Vynnycky, E., White, R.: An Introduction to Infectious Disease Modelling. Oxford University Press (2010)
2. Kabli, K., El Moujaddid, S., Niri, K., Tridane, A.: Cooperative system analysis of the Ebola virus epidemic model. Infect. Dis. Modell. **3**, 145–159 (2018)
3. WHO: Ebola disease factsheets. https://www.who.int/news-room/fact-sheets/detail/ebola-disease. Accessed April 2025
4. Kengne, J.N., Tadmon, C.: Ebola virus disease model with a nonlinear incidence rate and density dependent treatment. Infect. Dis. Model. **9**, 755–804 (2024)
5. Njankou, S.D.D., Nyabadza, F.: Modelling the potential influence of human migration and two strains on Ebola virus disease dynamics. Infect. Dis. Model. **7**, 645–659 (2022)
6. Juga, M.L., Nyabadza, F., Chirove, F.: An Ebola virus disease model with fear and environmental transmission dynamics. Infect. Dis. Modell. **6**, 545–559 (2021)
7. Gatherer, D.: The 2014 Ebola virus disease outbreak in West Africa. J. Gen. Virol. **95**(8), 1619–1624 (2014)
8. Medjoudja, M., El Hadi Mezabia, M., Riaz, M.B., Boudaoui, A., Ullah, S., Awwad, F.A.: A novel computational fractional modeling approach for the global dynamics and optimal control strategies in mitigating marburg infection. Aims Math. **9**(5), 13159–13194 (2024)
9. El Mesady, A., Elsadany, A.A., Mahdy, A.M.S., Elsonbaty, A.: Nonlinear dynamics and optimal control strategies of a novel fractional order lumpy skin disease model. J. Comput. Sci. **79**, 102286 (2024)
10. Elsonbaty, A., El Mesady, A.: Fractional order model for two strain monkeypox virus analytical and numerical insights with optimal control strategies. Part. Differ. Equ. Appl. Math. 101229, (2025)
11. Megala, T., Nandha Gopal, T., Siva Pradeep, M., Sivabalan, M., Yasotha, A.: Dynamics of re infection in a hepatitis B virus epidemic model with constant vaccination and preventive measures. J. Appl. Math. Comput. 1–27 (2025)
12. Saravanan, V., Chinnathambi, R., Rihan, F.A.: Modeling and controlling leptospirosis transmission in humans and rodents. J. Math. Comput. Sci. **39**(1), 30–49 (2025)
13. Peter, O.J., Babasola, O., Ojo, M.M., Omame, A.: A mathematical model for assessing the effectiveness of vaccination in controlling mpox dynamics and mitigating disease burden in Nigeria and the democratic Republic of Congo. J. Appl. Math. Comput. **71**, 5729–5756 (2025)

14. El Mesady, A., Ali, H.M.: The influence of prevention and isolation measures to control the infections of the fractional chickenpox disease model. Math. Comput. Simul. **226**, 606–630 (2024)
15. Balakrishnan, G.P., Chinnathambi, R., Rihan, F.A.: A fractional-order control model for diabetes with restraining and time delay. J. Appl. Math. Comput. **69**(4), 3403–3420 (2023)
16. Mohammadaliee, B., Samei, M.E., Roomi, V., Rezapour, S.: Optimal control strategies and cost effectiveness analysis for infectious diseases under fractal fractional derivative a case study of cholera outbreak. J. Appl. Math. Comput. **71**(3), 4197–4226 (2025)
17. Nasrin, S.F., Rajivganthi, C.: Dynamical analysis of a stochastic ebola Model with nonlinear incidence functions. J. Nonlinear. Sci. **35**(1), 33 (2025)
18. Xie, M., Younas Khan, M., Ullah, S., Farooq, M., Riaz, M.B., Alwan, B.A.: Optimal control analysis for the transmission of Nipah infection with imperfect vaccination. PLoS One **20**(4), e0317408 (2025)
19. Pal, K.K., Rai, R.K., Tiwari, P.K., Misra, A.K.: Mathematical modeling of control measures for preventing kidney failure and managing diabetes sensitivity analysis and optimal strategies. J. Appl. Math. Comput. 1–33 (2025)
20. Khan, M.Y., Ullah, S., Farooq, M., Riaz, M.B.: Modeling the dynamics of dengue fever with double susceptibility and optimal control strategies. Model. Earth Syst. Environ. 1–21 (2024)
21. Kamara, A.A., Wang, X., Tarus, S.K.: Global analysis of an environmental and death transmission model for Ebola outbreak with perturbation. Indian J. Pure Appl. Math. **52**(4), 1093–1105 (2021)
22. Lin, Q., Musa, S.S., Zhao, S., He, D.: Modeling the 2014 2015 Ebola virus disease outbreaks in Sierra Leone, Guinea, and Liberia with effect of high and low risk susceptible individuals. Bull. Math. Biol. **82**(8), (2020)
23. Kamara, A.A., Wang, X., Mouanguissa, L.N.: Analytical solution for post death transmission model of Ebola epidemics. Appl. Math. Comput. **367**, 124776 (2020)
24. Abah, R.T., Zhiri, A.B., Oshinubi, K., Adeniji, A.: Mathematical analysis and simulation of ebola virus disease spread incorporating mitigation measures. Franklin Open **6** (2024), 100066 (2023)
25. Barua, S., Denes, A.: Global dynamics of a compartmental model to assess the effect of transmission from deceased. Math. Biosci. **364**, 109059 (2023)
26. Ullah, I., Ahmad, I., Ali, N., Haq, I.U., Idrees, M., Albalwi, M.D., Yavuz, M.: Mathematical modeling and analysis of Ebola virus disease dynamics implications for intervention strategies and healthcare resource optimization. Math. Comput. Appl. **29**(5), 94 (2024)
27. Tasse, A.J.O., Kubalasa, V.B., Tsanou, B.: Nonstandard finite difference schemes for some epidemic optimal control problems. Math. Comput. Simul. **228**, 1–22 (2025)
28. Driessche, P.V.D., Watmough, J.: Reproduction number and sub threshold endemic equilibria for compartmental models of disease transmission. Math. Bios. **180**, 29–48 (2002)
29. Diekmann, O., Heesterbeek, J.A.P., Roberts, M.G.: The construction of next generation matrices for compartmental epidemic models. Interface. Focus. **7**, 873–885
30. Al-Hdaibat, B., DarAssi, M.H., Ahmad, I., Altaf Khan, M., Algethamie, R.: Investigating tuberculosis dynamics under various control strategies a comprehensive analysis using real statistical. Data. Math. Mthds. Appld. Sci. (2025)
31. Ullah, S., Khan, M.A.: Modeling the impact of non pharmaceutical interventions on the dynamics of novel coronavirus with optimal control analysis with a case study. Chaos, Solitons Fractals. **139**, 110075 (2020)
32. Wei, D., Luo, X., Qin, Y.: Controlling bifurcation in power system based on LaSalle invariant principle. Nonlinear Dyn. **63**, 323–329 (2011)
33. Ferretti, F., Saltelli, A., Tarantola, S.: Trends in sensitivity analysis practice in the last decade. Sci. The Total Environ. **568**, 666–670 (2016)
34. Sargent, R.W.H.: Optimal control. J. Comput. Appl. Math. **124**(1–2), 361–371 (2000)

Authors and Affiliations

Qiuni Zhu[1] · Muhammad Asim[2] · Saif Ullah[2,3] · Sabila[2] · Arshad Alam Khan[2]

✉ Saif Ullah
saifullah.maths@uop.edu.pk

Muhammad Asim
muhammadasim2024@uop.edu.pk

Sabila
sabilamaths2024@uop.edu.pk

[1] Department of Gastroenterology, First Affiliated Hospital of Air Force Medical University, Xi'an, China

[2] Department of Mathematics, University of Peshawar, Peshawar, Pakistan

[3] Jadara University Research Center, Jadara University, Irbid, Jordan